Copy 5
RM L53G23

NACA

RESEARCH MEMORANDUM

TRANSONIC AERODYNAMIC CHARACTERISTICS OF AN NACA 64A006 AIRFOIL SECTION WITH A 15-PERCENT-CHORD LEADING-EDGE FLAP

By Milton D. Humphreys

Langley Aeronautical Laboratory
Langley Field, Va.

NATIONAL ADVISORY COMMITTEE FOR AERONAUTICS

WASHINGTON

September 1, 1953

NACA RM L53G23

NATIONAL ADVISORY COMMITTEE FOR AERONAUTICS

RESEARCH MEMORANDUM

TRANSONIC AERODYNAMIC CHARACTERISTICS OF AN NACA 64A006 AIRFOIL SECTION WITH A 15-PERCENT-CHORD LEADING-EDGE FLAP

By Milton D. Humphreys

SUMMARY

Airfoil section normal-force, drag, pitching-moment, flap-normal-force, and hinge-moment characteristics obtained at Mach numbers from 0.5 to 1.0 on an NACA 64A006 airfoil equipped with a 15-percent-chord leading-edge flap are presented. The results indicate that for Mach numbers up to 0.8 the effect of deflecting the leading-edge flap was in agreement with available low-speed data, in that the flap had little effect on the angle of attack for zero lift and was effective in increasing the normal-force coefficient at which the drag started to increase rapidly. In the Mach number range from 0.5 to 0.8 and for normal-force coefficients greater than 0.4, flap deflections produced large increases in the ratio of normal force to drag. At higher Mach numbers, flap deflections increased the drag coefficients at all values of the normal-force coefficient and the ratio of normal force to drag was decreased. For Mach numbers up to 0.8, leading-edge-flap deflections increased the normal-force coefficient for moment-coefficient divergence. The flap center of pressure remained essentially constant with flap deflection.

INTRODUCTION

Low-speed two-dimensional investigation of leading-edge flaps (ref. 1) has shown that deflecting the flap not only increased the maximum lift coefficient, but was also effective in increasing the lift coefficient at which the drag increased rapidly. No aerodynamic force- and moment-coefficient data are available on two-dimensional airfoils equipped with leading-edge flaps at high subsonic and transonic Mach numbers. However, an unsteady-flow investigation at transonic Mach numbers (ref. 2) revealed that the leading-edge flap was beneficial in reducing the high-pressure pulsations associated with leading-edge-flow separation on the thin NACA 64A006 section. Because of interest in the use of leading-edge flaps stimulated by these results, and because it was expected that some of the beneficial effects of the flap at low speeds would be retained at high subsonic Mach numbers, an investigation was conducted at transonic speeds to determine the effects of the leading-edge-flap deflection on the aerodynamic characteristics of an NACA 64A006 airfoil equipped with a 15-percent-chord leading-edge flap. Pressure-distribution and wake-survey data were obtained at Mach numbers from 0.5 to 1.0 at angles of attack from 0° to 10° and flap-deflection angles from 0° to -15°. The Reynolds number of the flow based on the model chord ranged from 1.2×10^6 to 1.7×10^6.

SYMBOLS

c_d	section drag coefficient
c_n	section normal-force coefficient
$c_{m_{c/4}}$	section pitching-moment coefficient about the quarter-chord axis
c_{n_f}	flap normal-force coefficient based on the flap chord
c_h	flap hinge-moment coefficient based on the flap chord
M	free-stream Mach number
P	pressure coefficient, increment of local pressure above free-stream pressure expressed in terms of stream dynamic pressure
α	angle of attack, deg
δ	leading-edge-flap angle of deflection from chord line of symmetrical section, deg (down deflection is negative)
$\left(\frac{\partial c_n}{\partial \alpha}\right)_\delta$	normal-force-curve slope

$\left(\frac{\partial c_n}{\partial \delta}\right)_\alpha$ rate of change of normal force with flap deflection

$\left(\frac{\partial \alpha}{\partial \delta}\right)_{c_n}$ rate of change of angle of attack with flap deflection

APPARATUS, MODELS, AND TESTS

The tests were conducted in the Langley 4- by 19-inch semiopen tunnel (fig. 1) described in reference 3. Air from the atmosphere is induced to flow through the entrance nozzle into the test section and out through the diffuser. The test-section Mach number is held constant for each test point by a variable-area throat located in a diffuser downstream from the test section (see choker in fig. 1). This variable-area throat permitted continuous control of an undisturbed flow in the test section at Mach numbers from 0.3 to 1.0. The tunnel Mach number was determined from calibrated orifices in the test chamber above and below the test section.

The data of this investigation are subject to jet-boundary corrections. The jet-deflection correction to the angle of attack is the major correction, which for an incompressible or low-speed flow is given by the expression $\alpha_{true} = \alpha_{test} - 1.85c_n$ (for the model-tunnel configuration of this investigation, ref. 4). Since the validity of the incompressible jet-deflection correction has not been established at high subsonic Mach numbers, no correction has been applied to the test results presented herein. The tunnel calibration and jet-boundary effects are discussed in more detail in reference 3.

The model investigated was an NACA 64A006 airfoil section with a 15-percent-chord leading-edge flap (fig. 2). The ordinates are given in reference 2. The model had both a span and a chord of 4 inches, with static-pressure orifices at 2.5-, 5-, 10-, 15-, 20-, 25-, 30-, 35-, 40-, 45-, 50-, 55-, 60-, 65-, 70-, 75-, 80-, 85-, and 90-percent-chord stations on both upper and lower surfaces. The flap-hinge gap was unsealed and was held to 0.12-percent chord to reduce air leakage and surface irregularity.

Section normal-force coefficients, pitching-moment, flap-hinge-moment, and flap-normal-force coefficients were obtained from pressure-distribution measurements. The pressure-distribution data were obtained on a mercury manometer and photographically recorded. The drag coefficients were determined from the total pressure defect measured in the wake 1 chord downstream of the model trailing edge. No drag data are presented for 10° angle of attack, since data obtained by wake survey for drag determinations at angles of 10° and above are considered unreliable. In addition, high-speed schlieren motion pictures of the flow past the model (obtained for the investigation reported in ref. 2) were used as an aid for interpreting and analyzing the data. The data were obtained at Mach numbers from 0.5 to 1.0 for angles of attack from 0° to 10° and flap-deflection angles from 0° to -15°. The Reynolds number of the flow based on model chord ranged from 1.2×10^{6} to 1.7×10^{6}.

RESULTS

Pressure distributions along the chord of the model at 0.5, 0.8, and 0.92 Mach numbers for several constant angles of attack and for flap deflections of 0° and -5° are shown in figure 3. Figure 4 presents pressure distributions and the corresponding schlieren motion pictures of the flow about the model.

The basic data plots (fig. 5) show the variation of the section normal-force, drag, and pitching-moment coefficients with Mach number for several angles of attack and flap deflections. The corresponding coefficients for the flap based on the flap chord are presented in figure 6. The variation of section normal-force coefficient with angle of attack at constant Mach number and at several flap deflections is given in figure 7. The slopes of the normal-force curve are plotted as functions of Mach number in figure 8. Figure 9 presents the flap-effectiveness parameters $\left(\frac{\partial \alpha}{\partial \delta}\right)_{c_n}$ and $\left(\frac{\partial c_n}{\partial \delta}\right)_{\alpha}$ as functions of Mach number. The drag characteristics at constant angles of attack and flap deflections are presented in the form of polars in figure 10 and as ratios of normal force to drag in figure 11. The variations in moment coefficient with normal-force coefficient at constant angles of attack and flap deflections are shown in figure 12. The flap force and moment characteristics are presented in figures 13 and 14.

DISCUSSION

The variation of pressure along the surface of the model for flap deflections of 0° and -5° at various angles of attack and Mach numbers is presented in figure 3. These data show that the flap has a variable effect on the distribution of pressures on the surfaces over the forward portion of the airfoil that is dependent upon Mach number and angle of attack. The decrement in load that occurs near the nose with a downward deflection of the flap is observed in the pressure distributions through the Mach number and angle-of-attack ranges except at the high angles of attack and at the lower Mach numbers, where, at a Mach number of 0.5 and angle of attack of 8°, the 5° flap deflection produces an increase in the load on the nose of the profile (fig. 3(a)). Similar effects are noted at 10° angle of attack at Mach numbers of 0.5 and 0.8. At these Mach numbers the increment in load is a beneficial effect of the flap in eliminating the flow separation from the leading edge, as illustrated in figure 4 by the flow photographs and corresponding pressure distributions.

Generally, the decrement in load produced by the flap deflections over the forward part of the flap is compensated for to some extent by an increment in load over the rear of the flap and the forward part of the airfoil. This increment, however, is limited to lower angles of attack and the angle-of-attack range diminishes with increasing Mach number. At a Mach number of 0.92, the effects are only observed up to 4° angle of attack; at 6° the increment in load does not occur.

Normal-force coefficients.- The normal-force characteristics from the basic-data plots of figure 5 are cross-plotted in figure 7 to show the effect of flap deflection on the normal-force coefficients over the angle-of-attack range at each of several given Mach numbers. The data indicated that the angle of attack for zero lift at low Mach numbers is not appreciably affected by flap deflection, because of the compensating increment in load over the forward part of the profile as shown by the pressure-distribution data. The normal-force-curve slopes shown in figure 8 were obtained by using only that portion of the normal-force curves between 0° and 5° angle of attack. Generally, the normal-force-curve slope decreased with increasing flap deflection in the normal-force-coefficient range up to 0.5. At normal-force coefficients of 0.7 and above, deflection of the flap delayed the initial break in the normal-force curve and resulted in higher normal forces at a given angle of attack, and, consequently, higher normal-force-curve slopes. This is the result that would be expected from both the pressure-distribution data schlieren observations and previous low-speed tests on flaps. This general behavior is maintained up to Mach numbers of approximately 0.8, where the larger flap deflection $\left(-15^{\circ}\right)$ becomes definitely inferior to the basic profile. The general increase with Mach number of the normal-force coefficient at which flap deflection begins to improve the normal force (observed at Mach numbers from 0.5 to 0.8) results in no beneficial effect of the flap above a Mach number of 0.9.

At the lower Mach numbers and moderately high angles of attack, improvement in the normal-force characteristics of the profile as a result of flap deflection was shown by schlieren photographs to be a result of the alleviation of the separated-flow condition. Previous investigations of both the basic profile and of unsteady flows have shown that with increasing Mach number, at a given angle of attack, flow attachment would occur and alleviate the flow separation near the leading edge (ref. 5). Studies of the unsteady flow indicated that the attachment was not a sudden occurrence, but was an oscillatory phenomenon that persisted over a small Mach number range (about 0.02). The Mach number at which flow attachment occurred increased with increasing angle of attack and was about 0.67 at 6°, 0.7 at 8°, and 0.8 at 10°. The flow attachment which occurred at the higher Mach number on the basic profiles accomplished the same purpose as the flap did at low Mach numbers, and thus the flap was rendered not only ineffective, but actually detrimental in the high Mach number range.

Flap effectiveness.- Flap effectiveness, expressed either as the rate of change of normal force with flap deflection $\left(\frac{\partial c_n}{\partial \delta}\right)_\alpha$ or the ratio of that quantity to the normal-force-curve slope with angle of attack, expressed as $\left(\frac{\partial \alpha}{\partial \delta}\right)_{c_n}$ (fig. 9), can be determined theoretically for an incompressible potential flow and is 0.0027 and 0.025, respectively. These values correspond to the reduction in normal-force-curve slope with downward deflection of the flap $(-\delta)$ which is observed at the lower angles of attack. An improvement in force characteristics as a result of flap deflection corresponds to negative values of flap effectiveness and coincides with the improved normal-force characteristics observed at the high angles of attack at Mach numbers less than 0.8 and is reflected in these flap-effectiveness parameters.

Drag characteristics.- Variation in the drag coefficient with normal-force coefficient as affected by flap deflection at constant angles of attack throughout the Mach number range (fig. 10) reflects the flow changes effected by the flap shown in the normal-force characteristics. At the high angles of attack and low Mach numbers, flap deflections produced large decreases in the drag coefficient. At Mach numbers above 0.8, throughout the normal-force-coefficient range, deflection of the flap at constant angles of attack increased the drag. The improved characteristics due to flap deflection are combined in figure 11 to produce very high n/d values for Mach numbers up to 0.8 and low values above 0.8. While the n/d ratios are highest for the basic model at Mach numbers of 0.85, 0.9, and 0.95, the increment in n/d resulting from deflecting the flap becomes progressively less as the Mach number increases and approaches 1.0.

Pitching-moment characteristics.- In accord with the low-speed data (ref. 1), the general slope of the pitching-moment coefficient with leading-edge-flap deflection at low Mach numbers and for normal-force coefficients up to 0.6 is negative (figs. 5 and 12). At normal-force coefficients up to around 0.6, increasing the Mach number from 0.5 to 0.8 produced increases in the negative moment coefficient due to leading-edge-flap deflection as a result of the general rearward shift in loading induced by the deflected flap and the large decrease in loading over the nose of the airfoil (figs. 3 and 6). For Mach numbers up to 0.8 in the high normal-force-coefficient range, deflection of the leading-edge flap produced a significant increase in the normal-force coefficient at which the moment coefficient diverged rapidly in a negative direction (fig. 12). The pressure-distribution diagrams (fig. 3) indicate that the increased loading over the leading-edge flap at high normal-force coefficients for the flap-deflected condition is responsible for the increase in the normal-force coefficient for moment divergence. The rates of change of pitching-moment coefficient with normal-force coefficient $\left(\frac{\partial c_{m_{c/4}}}{\partial c_n}\right)_\delta$ are generally small for Mach numbers up to around 0.85. At the higher Mach numbers the slopes become increasingly negative with increasing Mach number. The slopes of the curves for $\left(\frac{\partial c_{m_{c/4}}}{\partial c_n}\right)_\delta$ at low normal-force coefficients are not significantly affected by small deflections of leading-edge flap.

Flap hinge-moment and normal-force characteristics.- At high angles of attack (8° to 10°) and low Mach numbers (0.5 to 0.8) (fig. 6), where favorable effects of flap were observed on normal force and drag, the flap deflection alleviated the flow separation at the leading edge and produced increases in flap normal-force coefficient and flap hinge-moment coefficent. The changes in hinge-moment coefficient with flap normal-force coefficient (presented in fig. 13) for the various Mach numbers and flap deflections show a linear variation with little change in slope with either Mach number or flap deflection, thereby this variation indicates that the flap center of pressure remains essentially constant. In the subsequent discussion, therefore, any discussion of effects on hinge-moment coefficient pertains equally to flap normal-force coefficient.

At angles of attack less than 8° and at low Mach numbers, the data in figure 14 show that the rate of change in hinge-moment coefficient with section normal-force coefficient at constant angles of attack is very much larger than the slope at constant flap deflection. A comparison of the slopes of hinge moment with normal force includes $\left(\frac{\partial c_n}{\partial \alpha}\right)_\delta$ and $\left(\frac{\partial c_n}{\partial \delta}\right)_\alpha$, and figures 8 and 9 show that the $\left(\frac{\partial c_n}{\partial \delta}\right)_\alpha$ is only three percent of $\left(\frac{\partial c_n}{\partial \alpha}\right)_\delta$ at low angles of attack and low Mach numbers. Taking these factors into consideration, an evaluation of $\left(\frac{\partial c_h}{\partial \alpha}\right)_\delta$ and $\left(\frac{\partial c_h}{\partial \delta}\right)_\alpha$ shows that the rate of change of hinge moment with angle of attack is approximately five times the rate of change of hinge moment with flap deflection. From incompressible flow considerations, the change in hinge-moment coefficient with angle of attack may be considered the result of the change in loading on the leading edge that occurs with angle of attack which in incompressible flow is very large. The change in hinge moment with flap deflection, however, may be considered equal to the change in hinge moment with angle of attack minus the change in loading resulting from a downward deflection of the flap, which causes a considerable reduction in the load on the flap. The resulting effect makes the change in load due to the flap deflection relatively small at low speeds. It could be expected, however, that, as the Mach number is increased above the critical, the effect of deflections of the trailing portion of the airfoil on the load of the leading edge would diminish and the rate of change of hinge moment with angle of attack would decrease and would approach the value of the rate of change of hinge moment with flap deflection as Mach number 1 is approached, as shown by the data.

SUMMARY OF RESULTS

The results of a two-dimensional wind-tunnel investigation of the aerodynamic characteristics of an NACA 64A006 airfoil section equipped with a 15-percent-chord leading-edge flap indicated that:

1. For Mach numbers up to 0.8, the effect of deflecting the leading-edge flap was in agreement with available low-speed data, in that the flap had little effect on the angle of attack for zero lift and was effective in increasing the normal-force coefficient at which the drag started to increase rapidly.

2. In the Mach number range from 0.5 to 0.8, and for normal-force coefficients greater than 0.4, flap deflections produced large increases in the ratio of normal force to drag.

3. At Mach numbers greater than 0.8, flap deflections increased the drag coefficients at all values of the normal-force coefficient and the ratio of normal force to drag was decreased.

4. For Mach numbers up to 0.8, leading-edge-flap deflections increased the normal-force coefficient for moment-coefficient divergence.

5. The flap center of pressure remained essentially constant with flap deflection.

Langley Aeronautical Laboratory,
National Advisory Committee for Aeronautics,
Langley Field, Va., July 7, 1953.

REFERENCES

1. Nuber, Robert J., and Gottlieb, Stanley M.: Two-Dimensional Wind-Tunnel Investigation at High Reynolds Numbers of an NACA 65A006 Airfoil With High-Lift Devices. NACA RM L7K06, 1948.

2. Humphreys, Milton D., and Kent, John D.: The Effects of Camber and Leading-Edge-Flap Deflection on the Pressure Pulsations on Thin Rigid Airfoils at Transonic Speeds. NACA RM L52G22, 1952.

3. Daley, Bernard N., and Dick, Richard S.: Effect of Thickness, Camber, and Thickness Distribution on Airfoil Characteristics at Mach Numbers up to 1.0. NACA RM L52G31a, 1952.

4. Katzoff, S., Gardner, Clifford S., Diesendruck, Leo, and Eisenstadt, Bertram J.: Linear Theory of Boundary Effects in Open Wind Tunnels With Finite Jet Lengths. NACA Rep. 976, 1950. (Supersedes NACA TN 1826.)

5. Lindsey, W. F., Daley, Bernard N., and Humphreys, Milton D.: The Flow and Force Characteristics of Supersonic Airfoils at High Subsonic Speeds. NACA TN 1211, 1947.

[redacted]

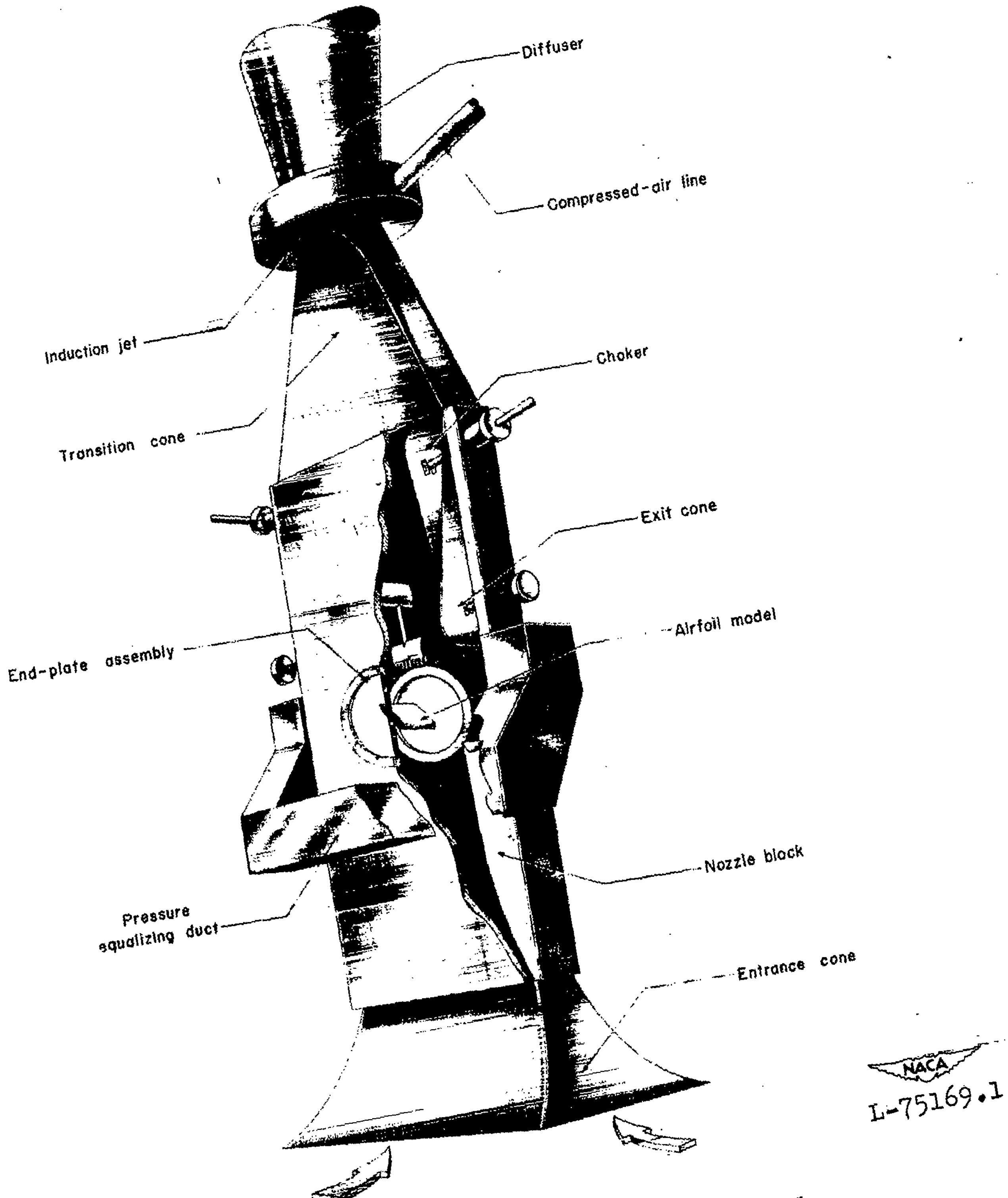

Figure 1.- Langley 4- by 19-inch semiopen tunnel.

[redacted]

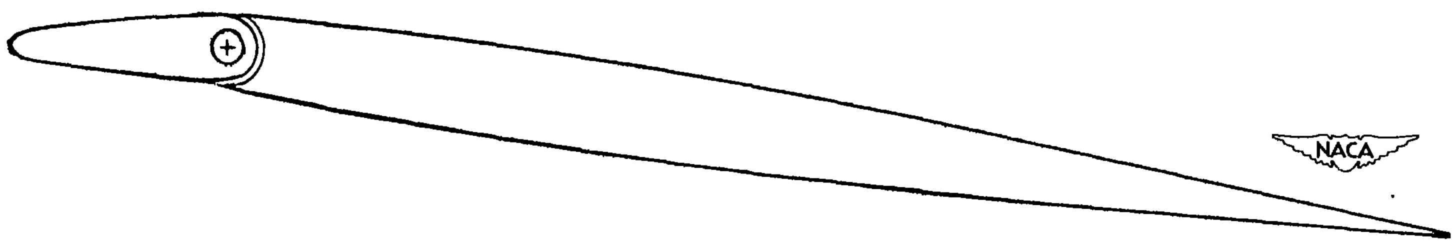

Figure 2.- The NACA 64A006 airfoil with 15-percent-chord leading-edge flap.

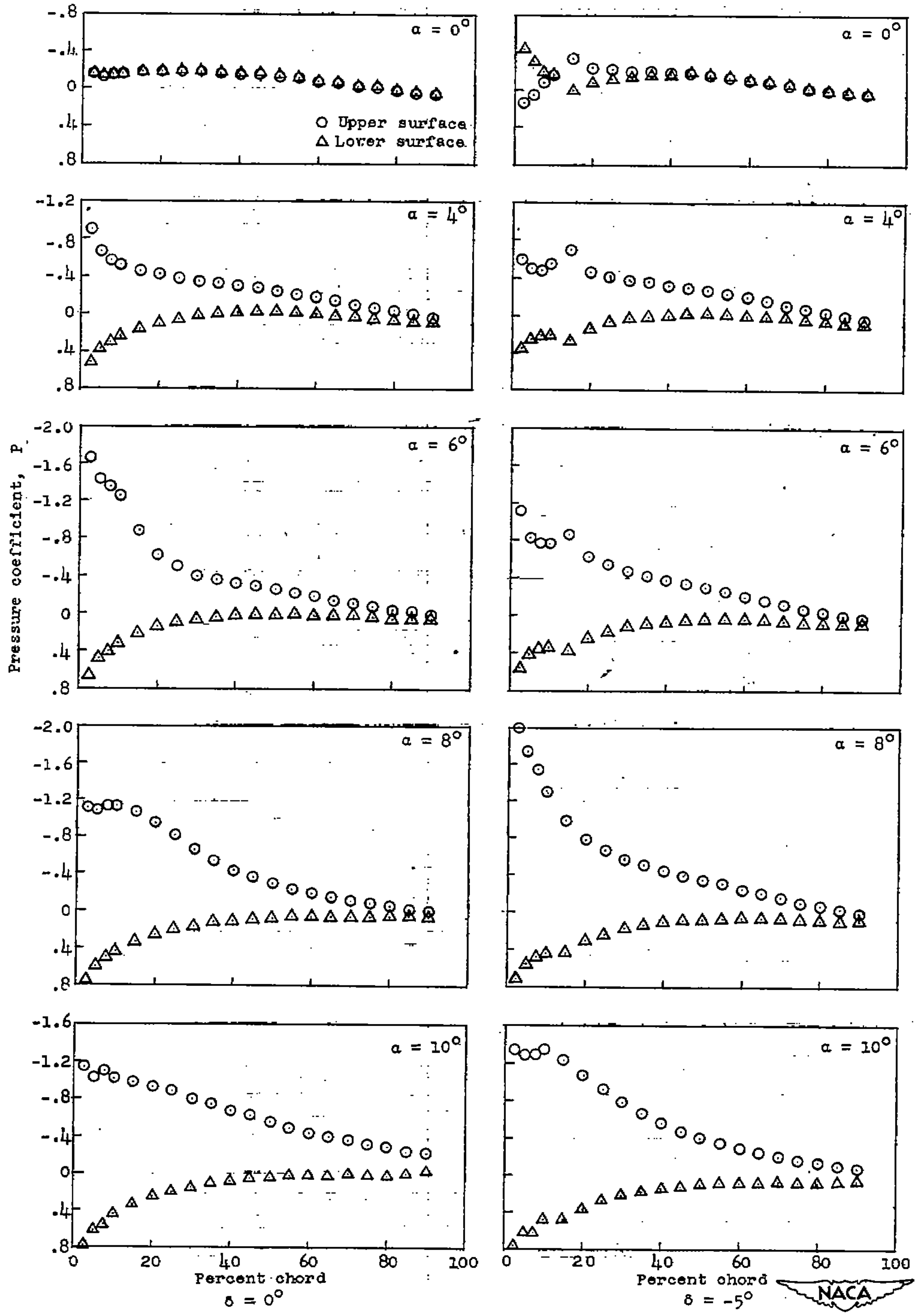

(a) M = 0.5.

Figure 3.- Effect of leading-edge-flap deflection on the pressure distributions at Mach numbers from 0.5 to 0.92.

[redacted]

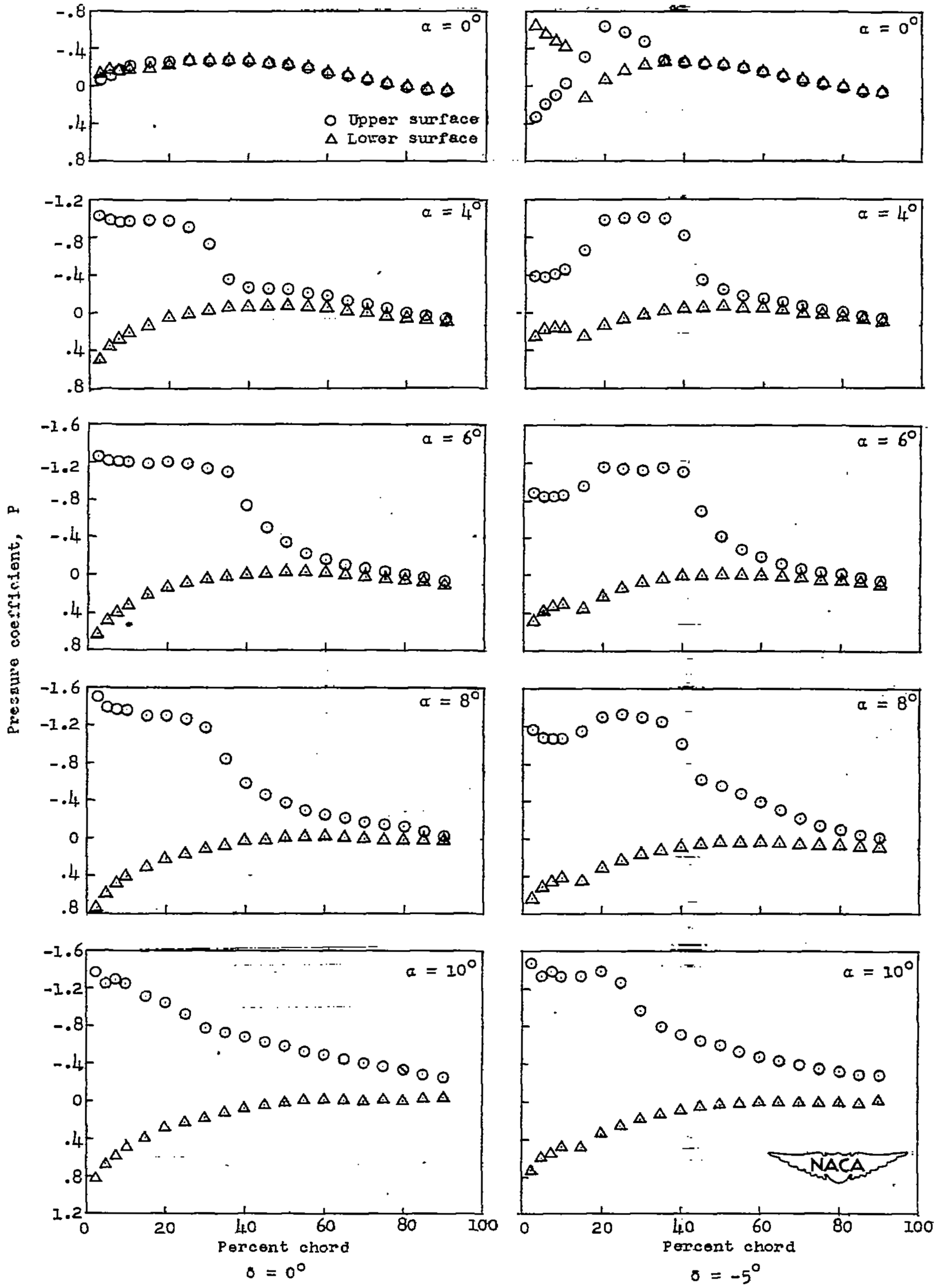

(b) M = 0.8.

Figure 3.- Continued.

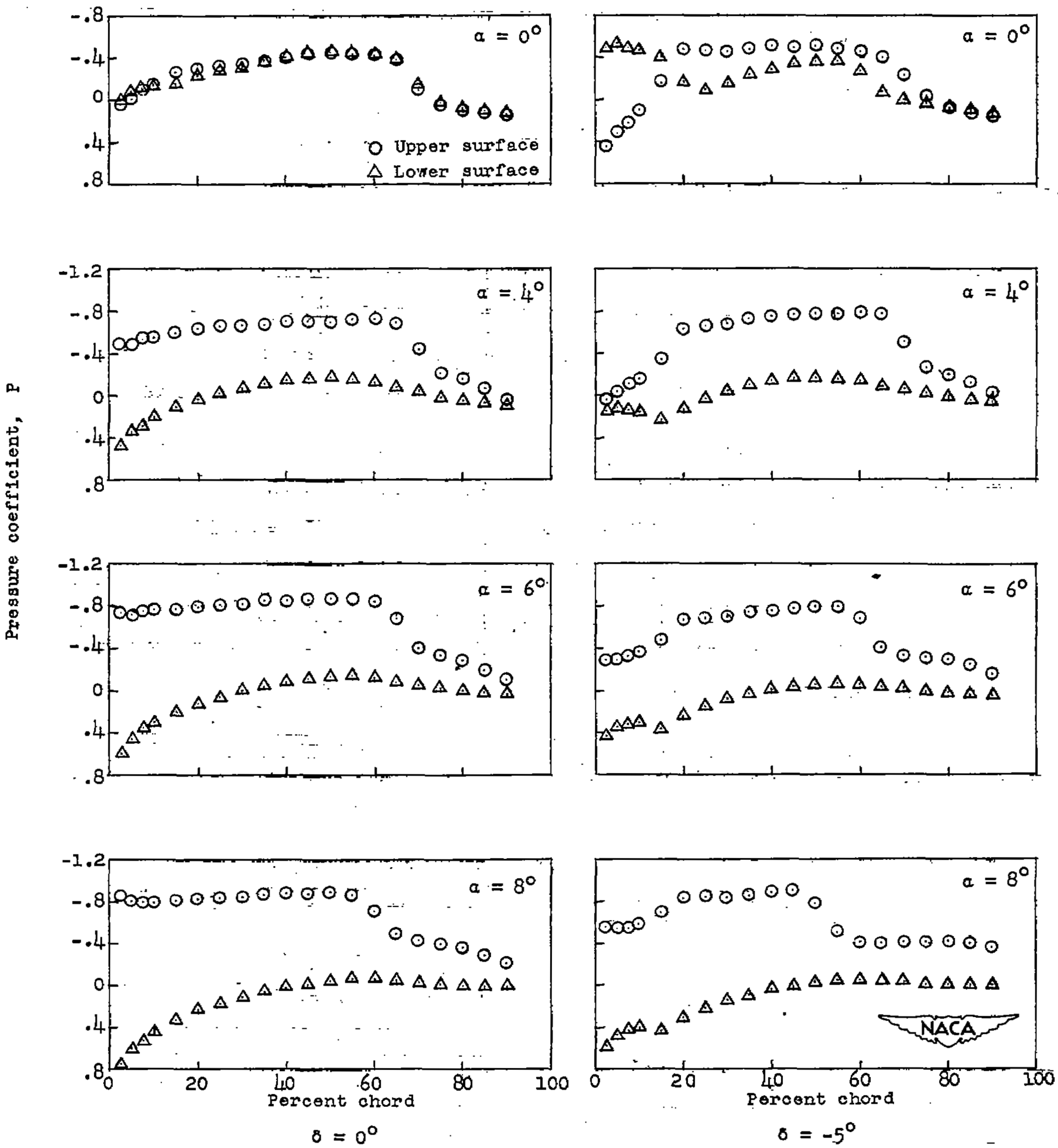

(c) M ≈ 0.92.

Figure 3.- Concluded.

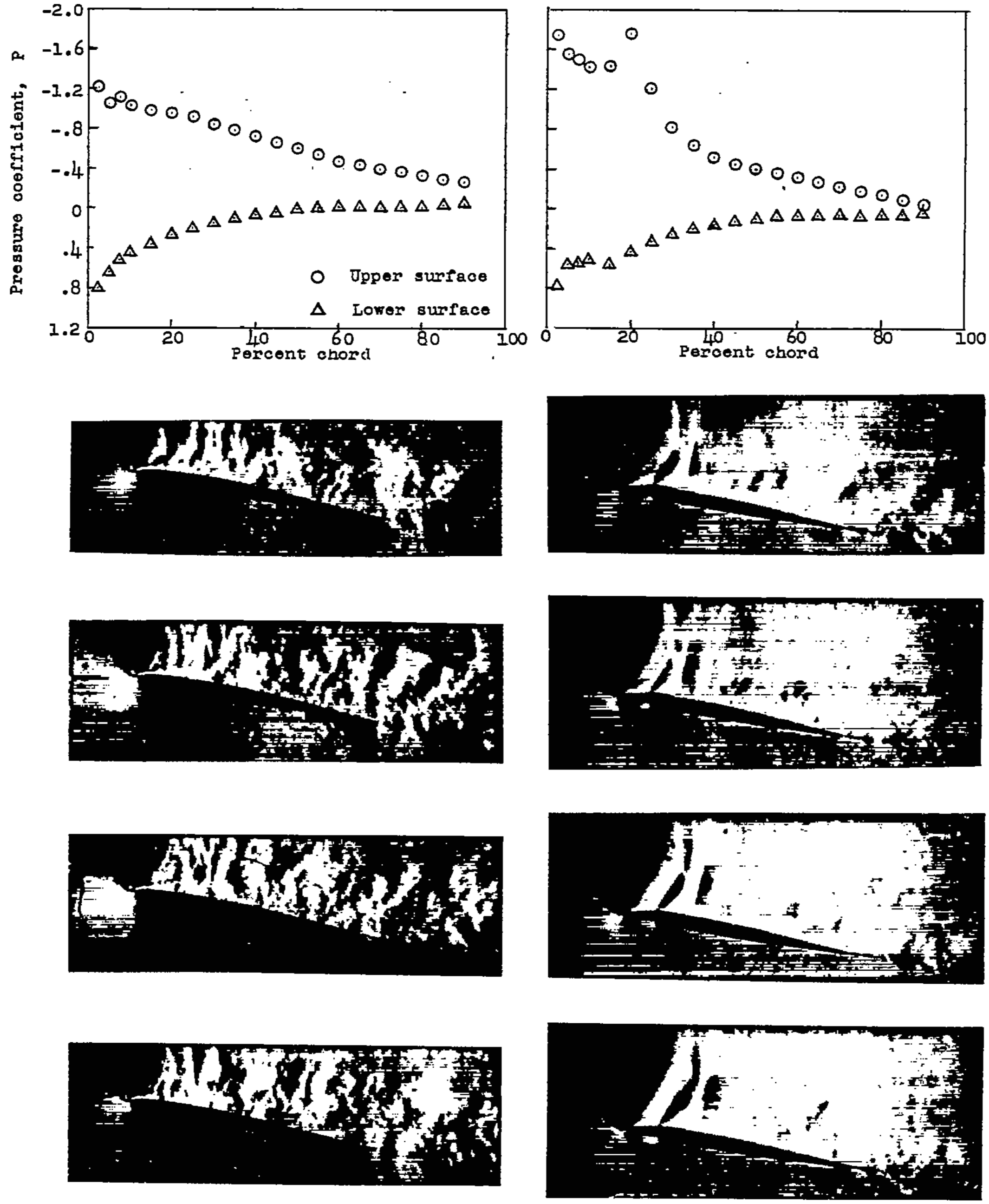

δ = 0°　　δ = -10°

NACA

L-80244

Figure 4.- Pressure distribution and corresponding schlieren high-speed motion-picture flow photographs (250 frames per second) at a Mach number of 0.7 and angle of attack of 10° for leading-edge-flap deflections of 0° and -10°.

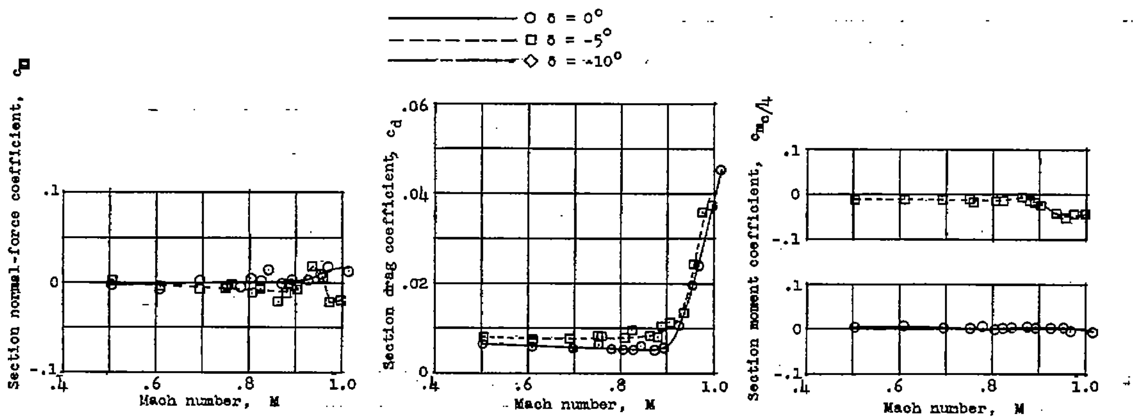

(a) α = 0°.

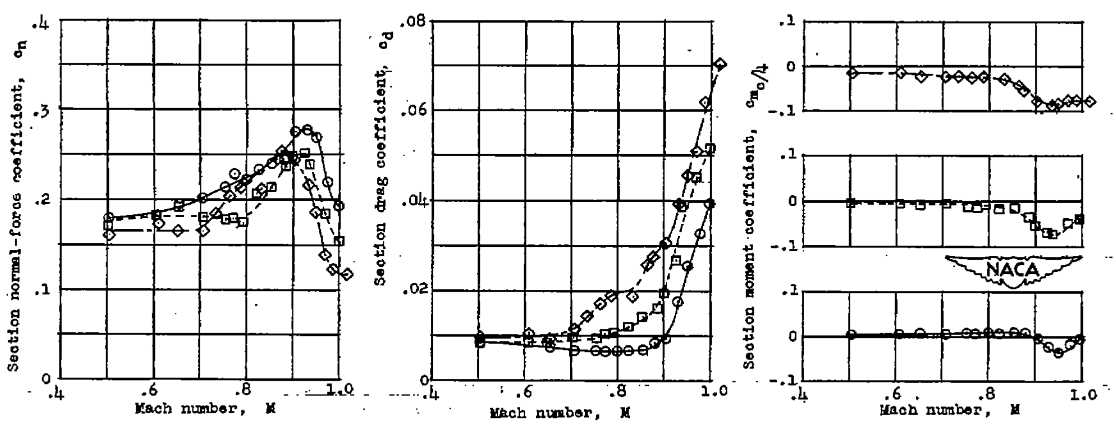

(b) α = 2°.

Figure 5.- Airfoil characteristics of the NACA 64A006 airfoil with 15-percent-chord leading-edge flap.

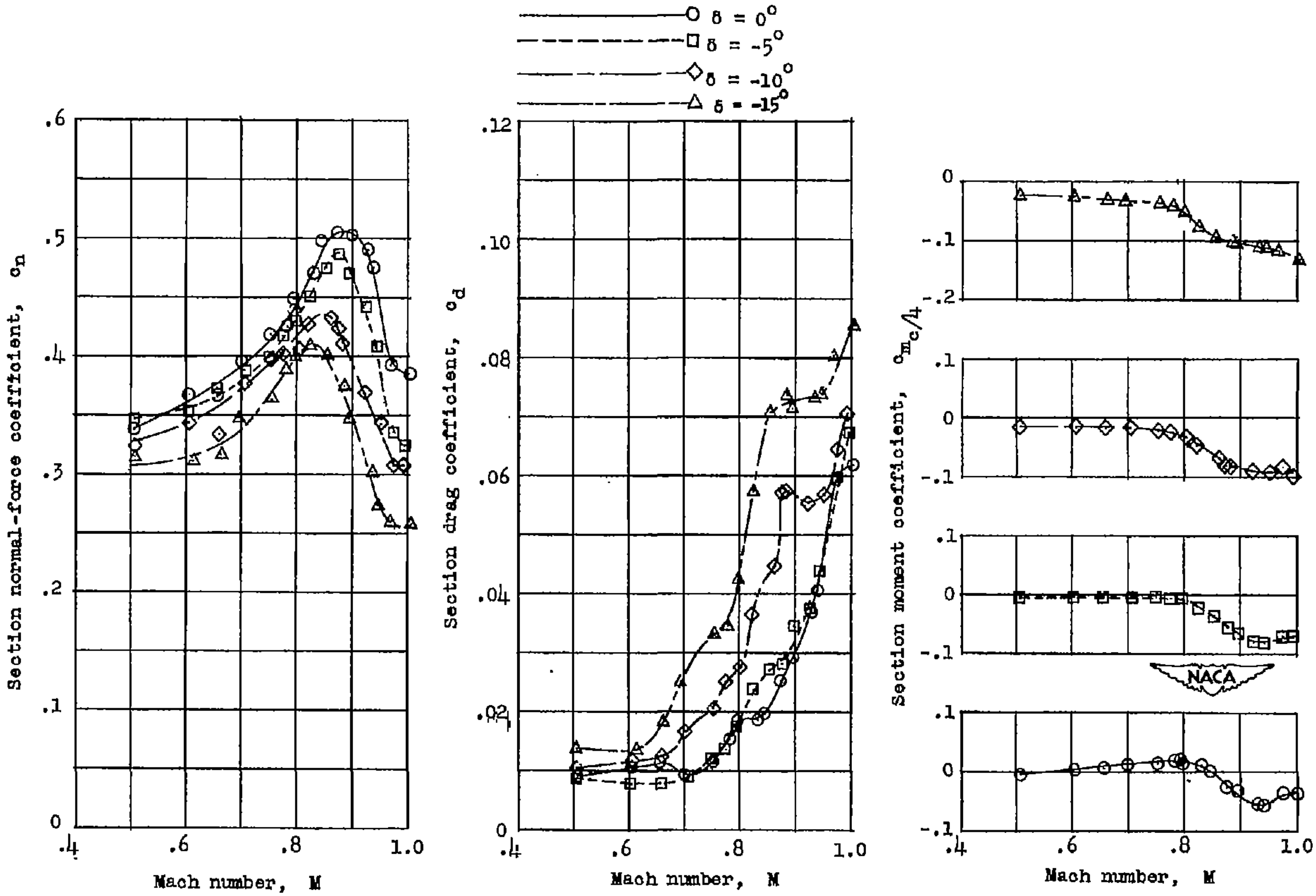

(c) $\alpha = 4^{\circ}$.

Figure 5.- Continued.

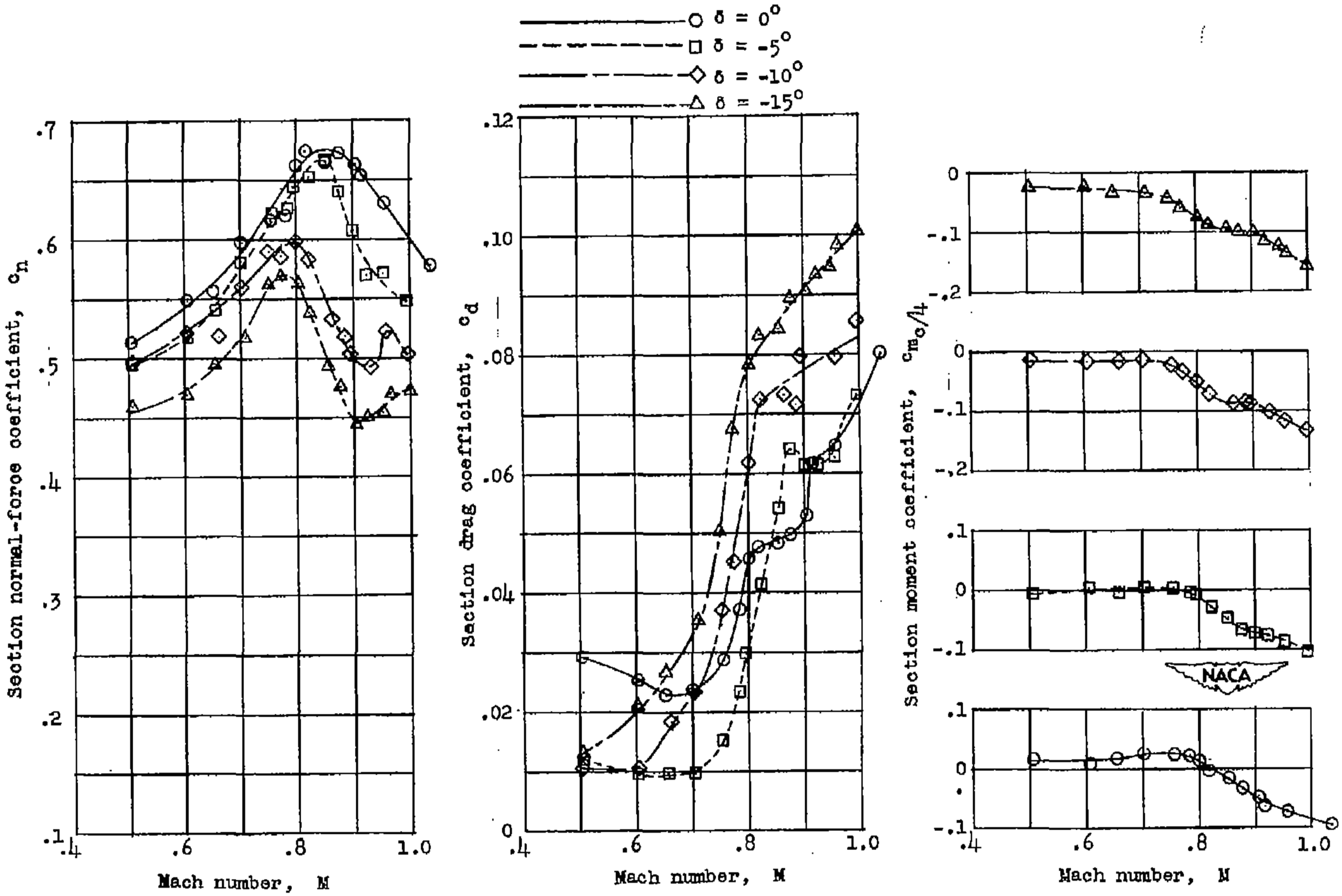

(d) $\alpha = 6^{\circ}$.

Figure 5.- Continued.

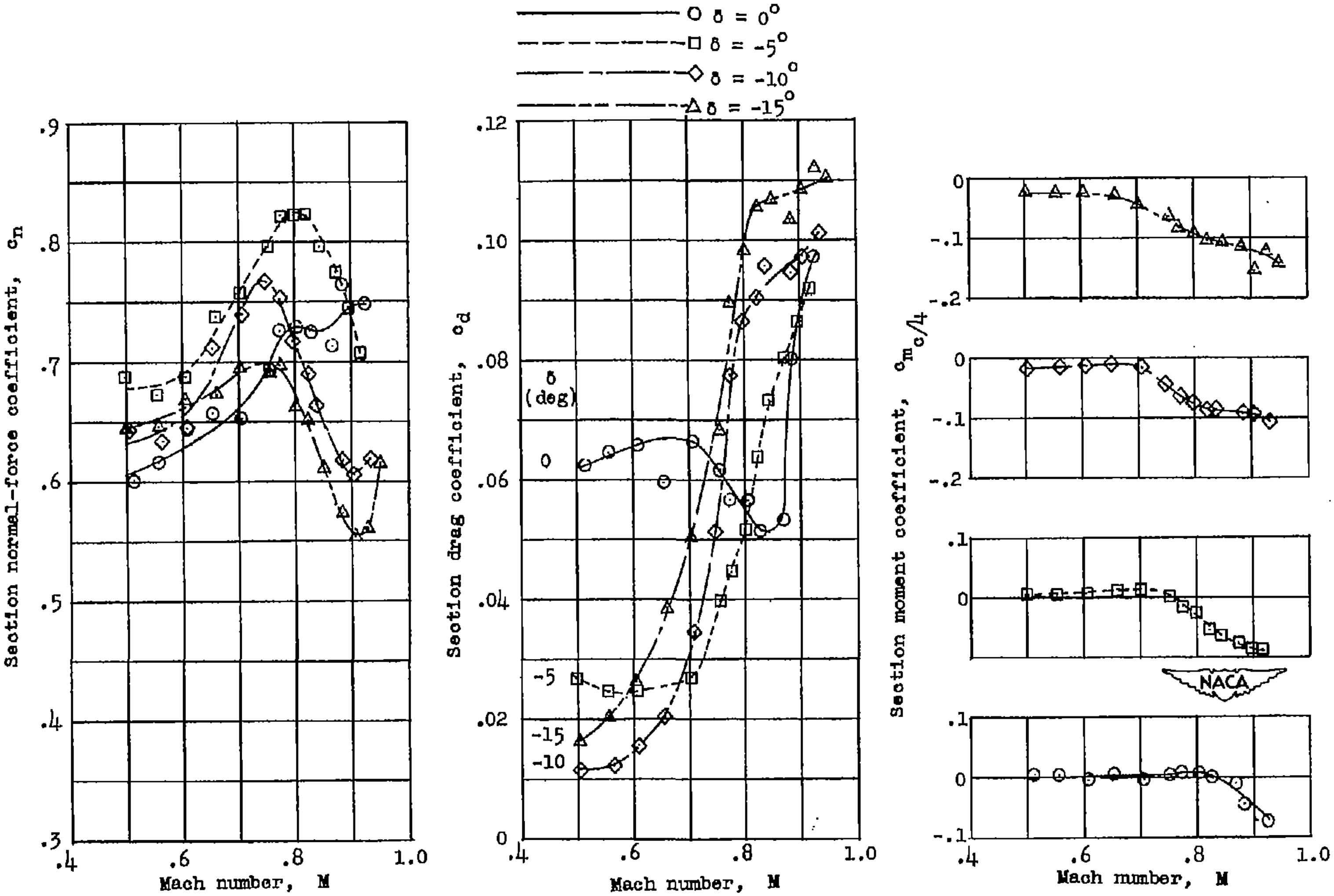

(e) $\alpha = 8^{\circ}$.

Figure 5.- Continued.

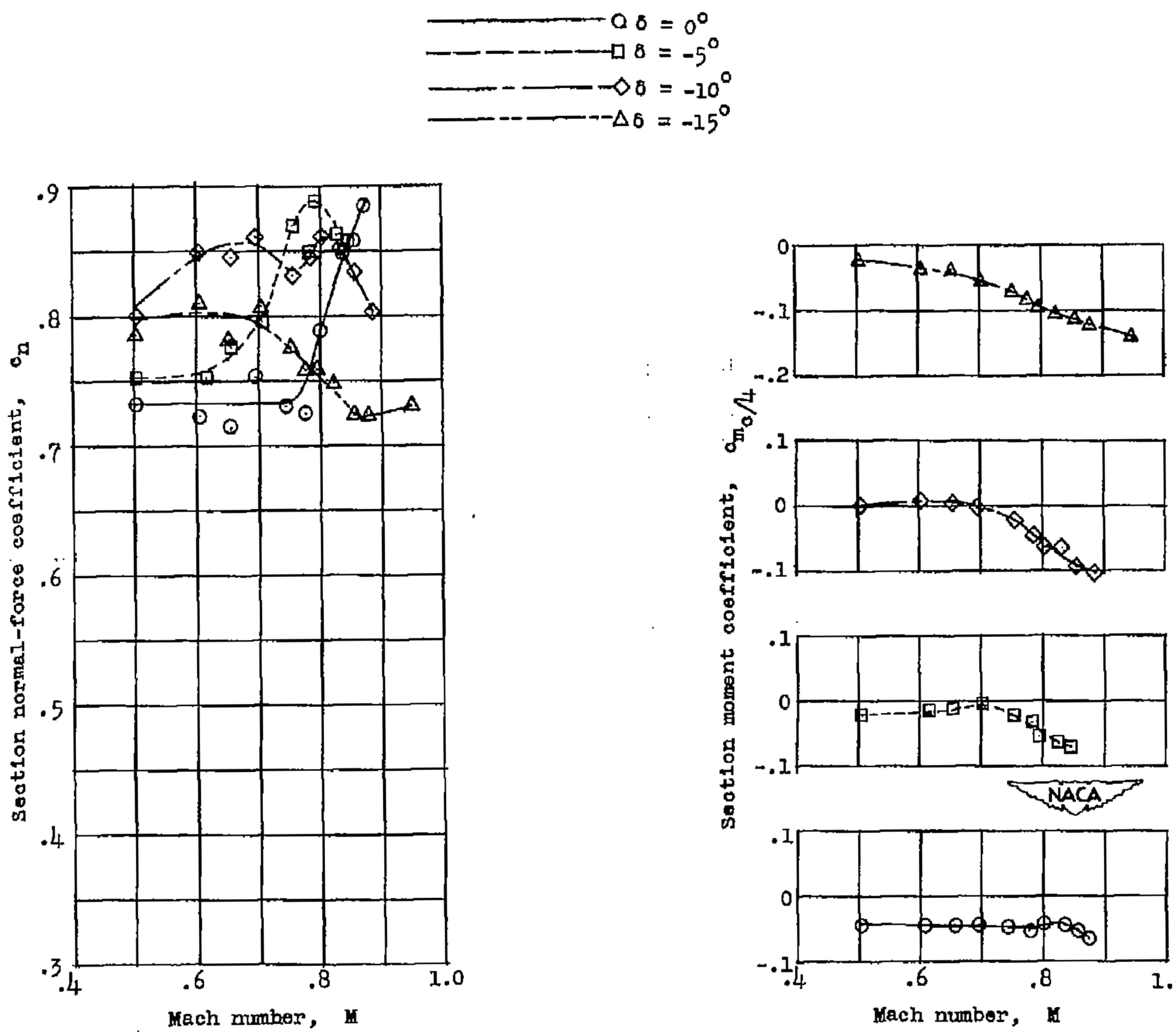

(f) $\alpha = 10°$.

Figure 5.- Concluded.

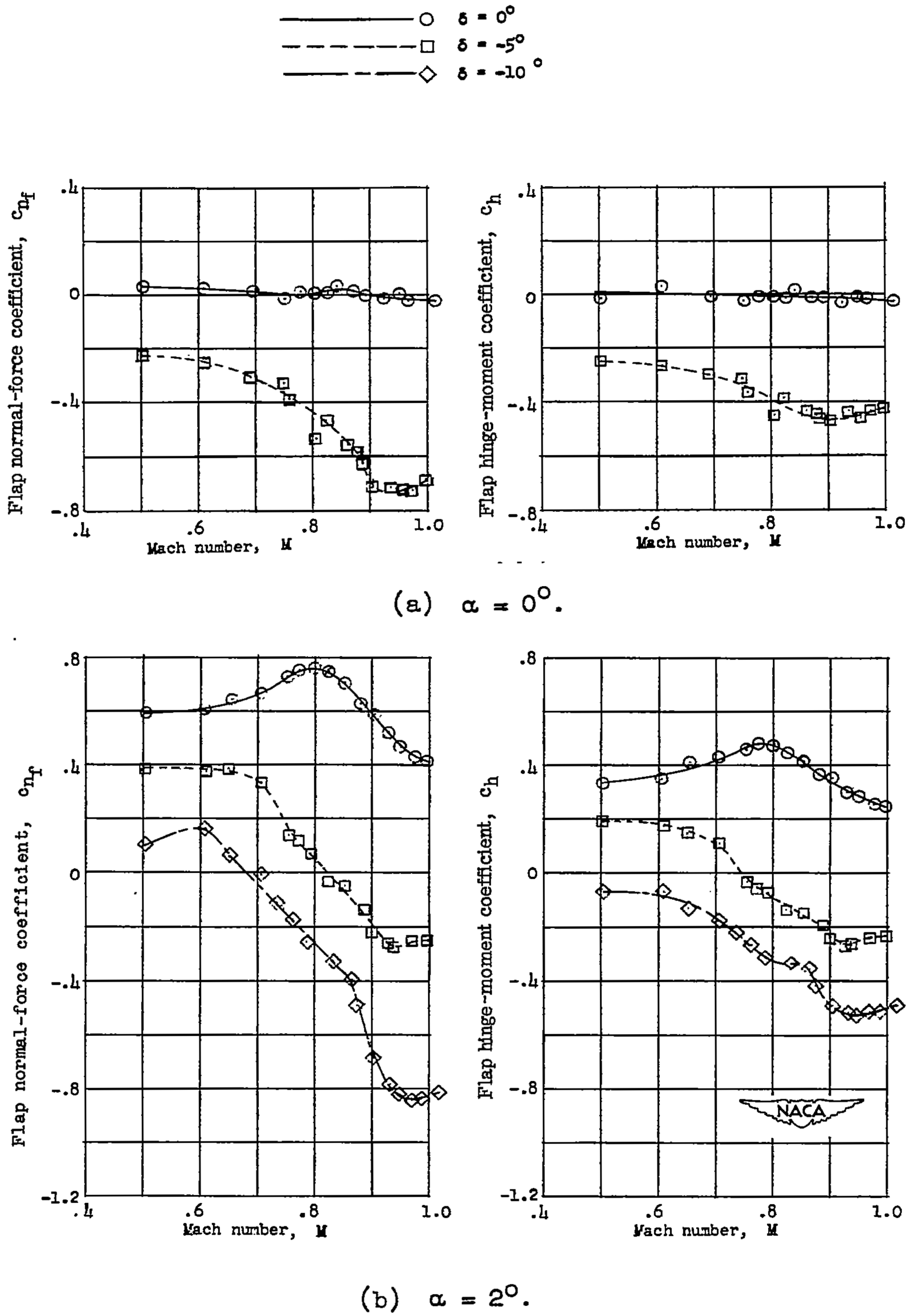

Figure 6.- Flap normal-force and hinge-moment coefficients for the NACA 64A006 airfoil with 15-percent-chord leading-edge flap.

[redacted]

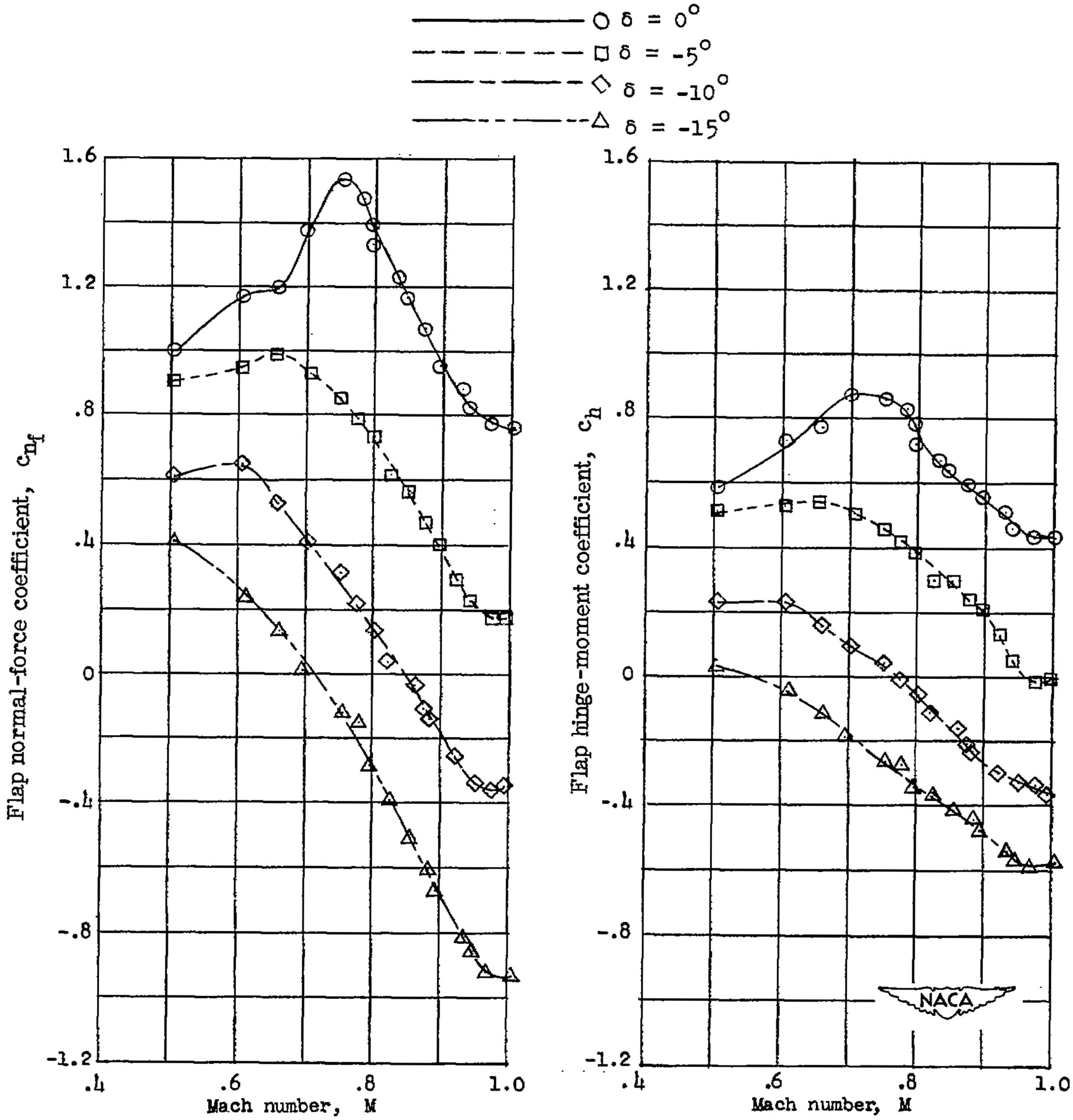

(c) $\alpha = 4^{\circ}$.

Figure 6.- Continued.

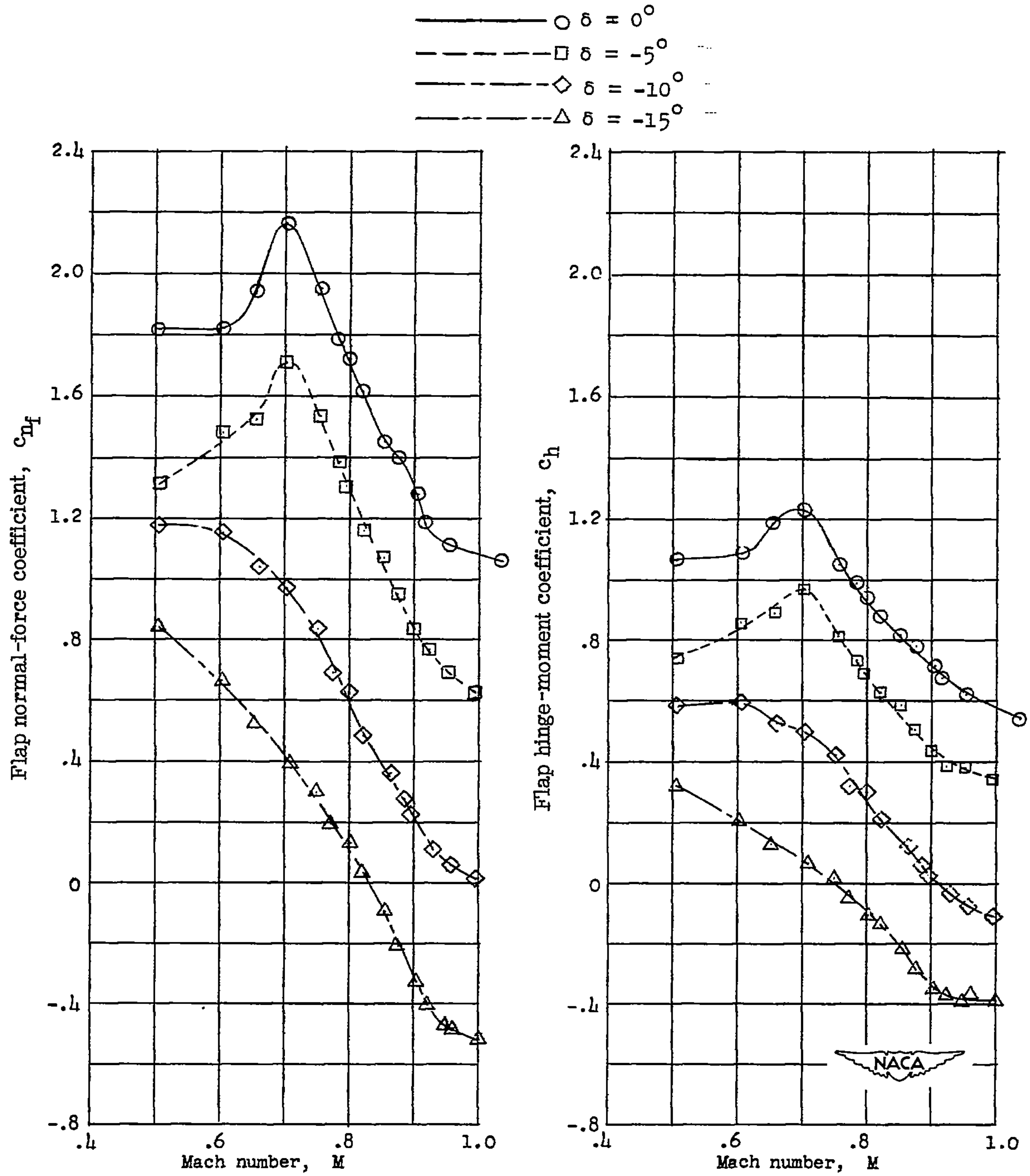

(d) $\alpha = 6^{\circ}$.

Figure 6.- Continued.

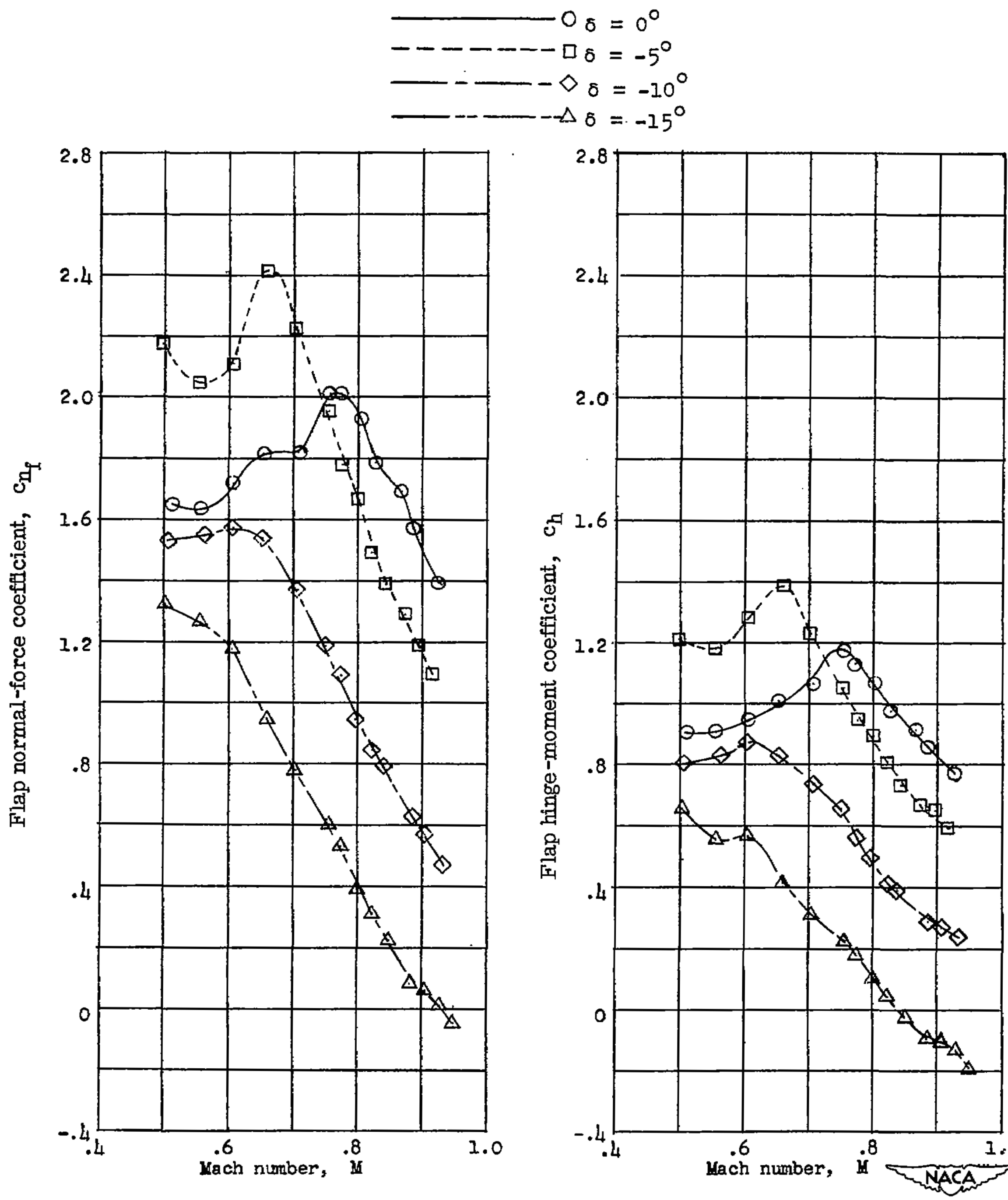

(e) $\alpha = 8^\circ$.

Figure 6.- Continued.

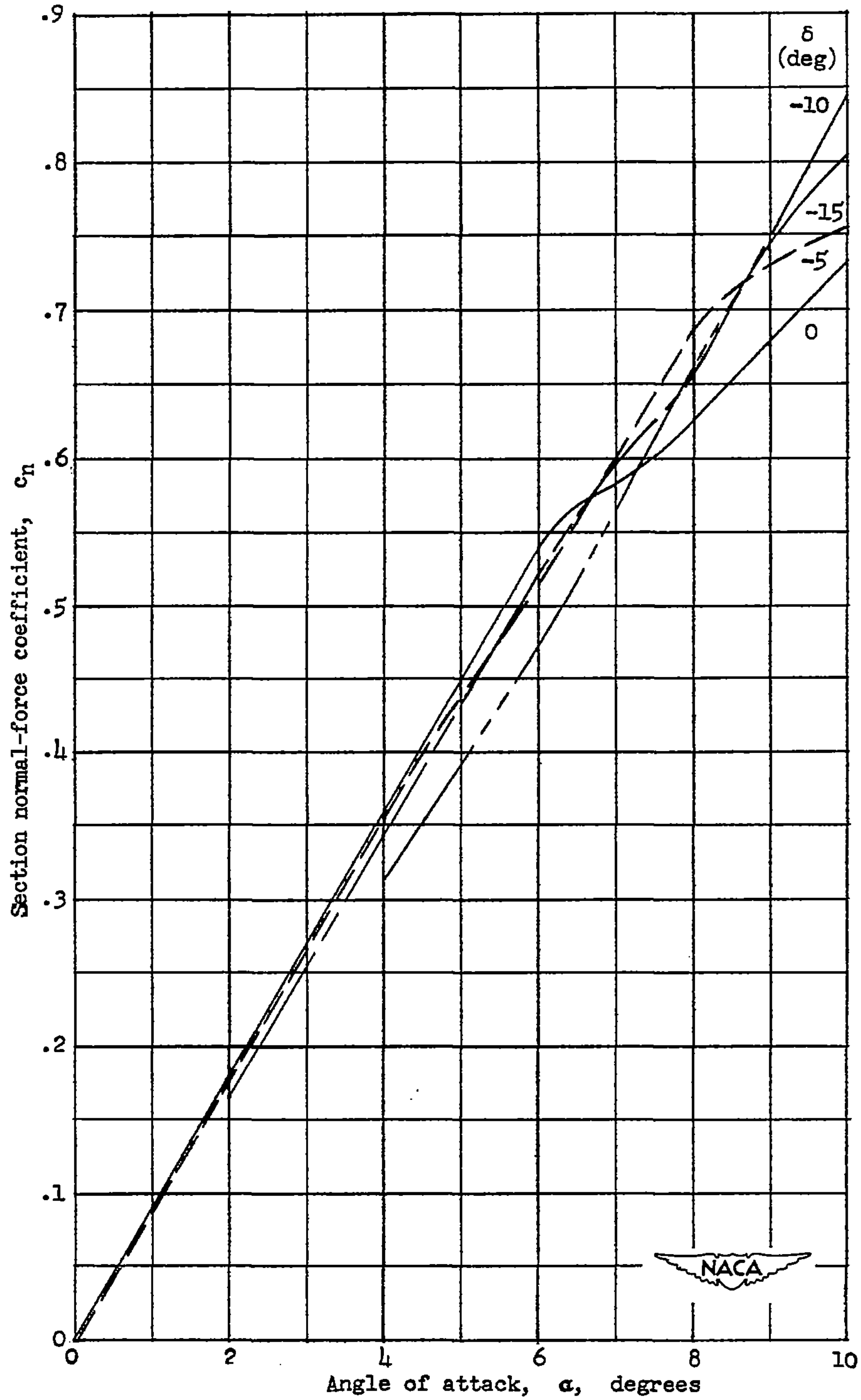

(b) $M = 0.6$.

Figure 7.- Continued.

[redacted]

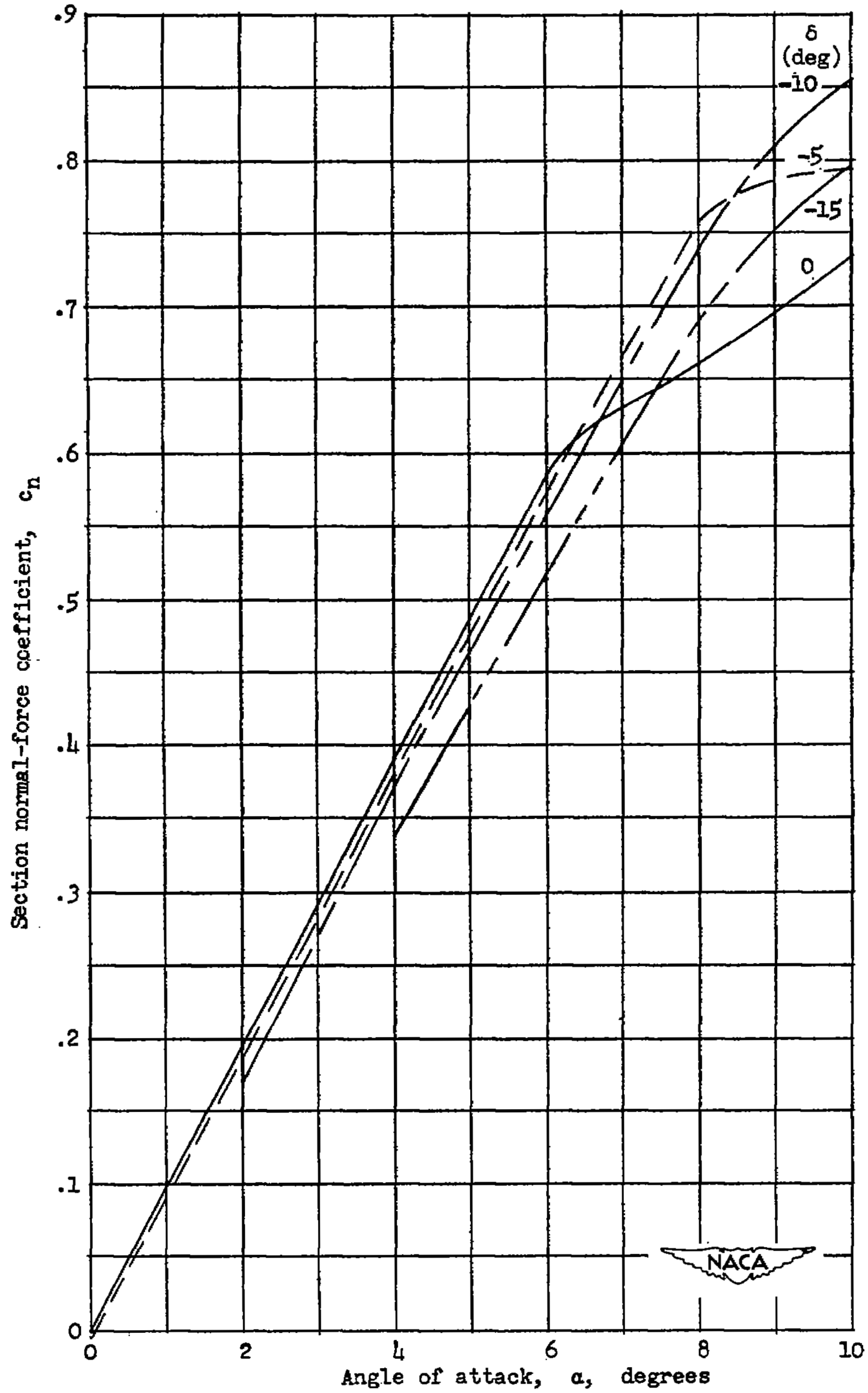

(c) M = 0.7.

Figure 7.- Continued.

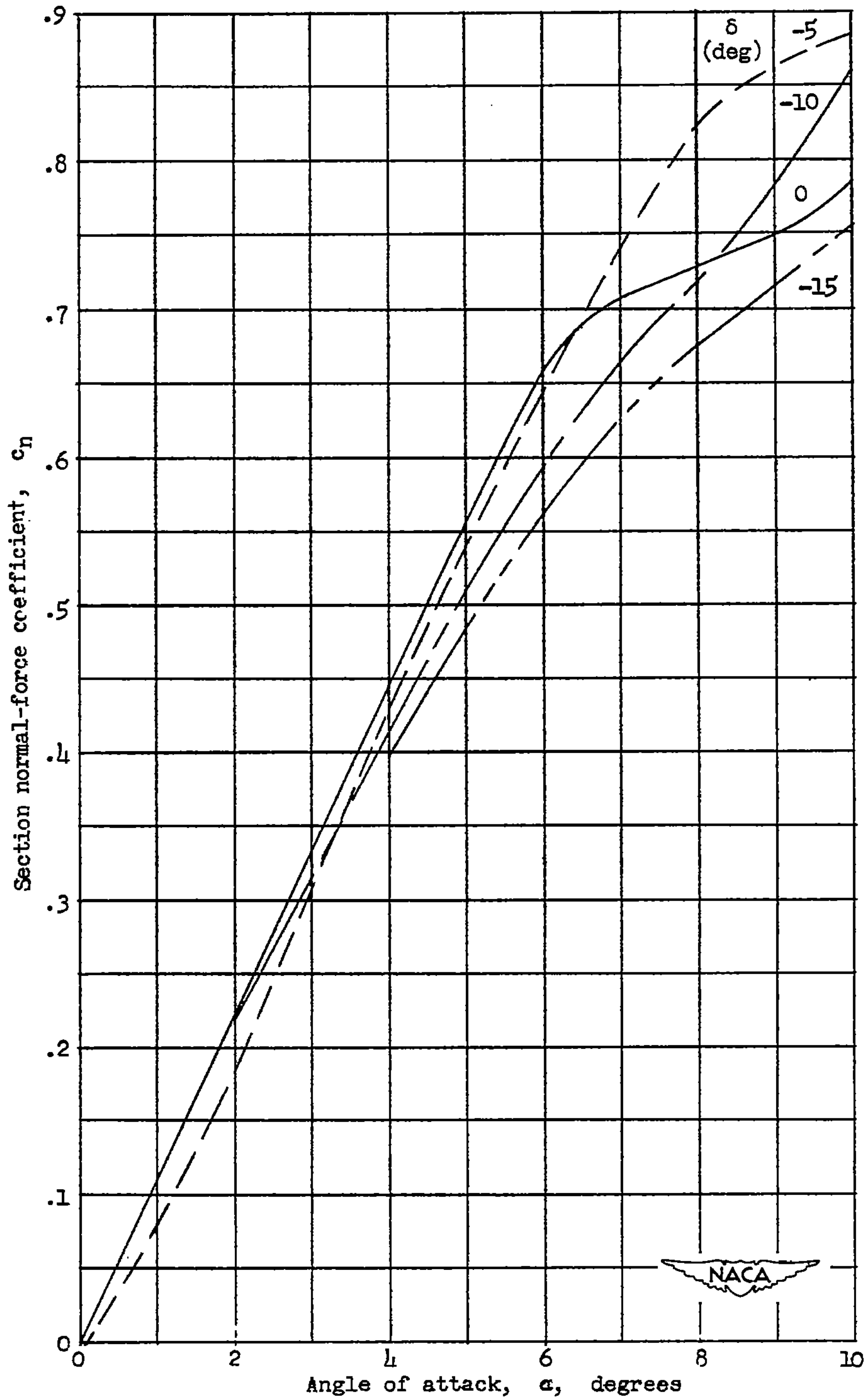

(d) M = 0.8.

Figure 7.- Continued.

[redacted]

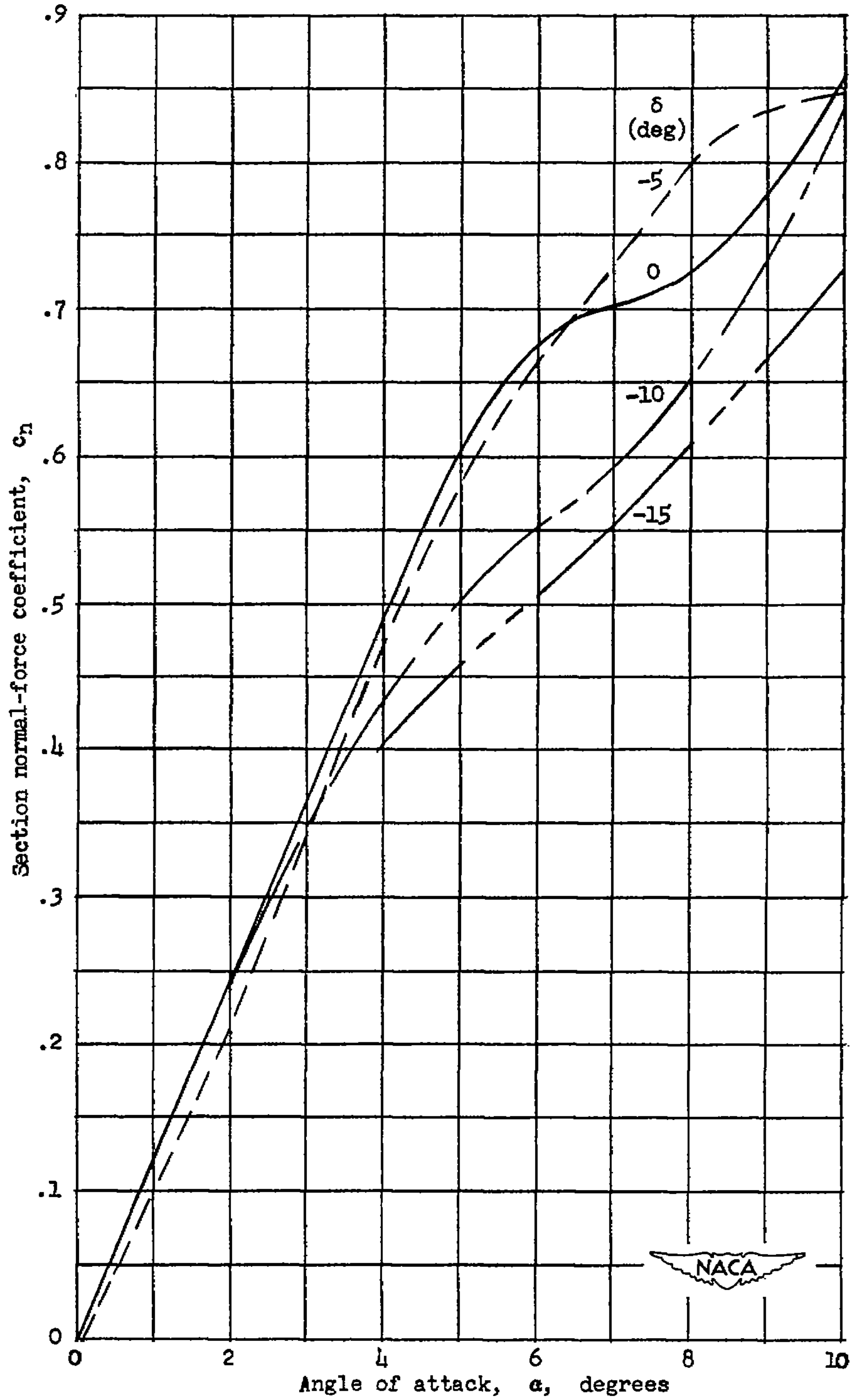

(e) M = 0.85.

Figure 7.- Continued.

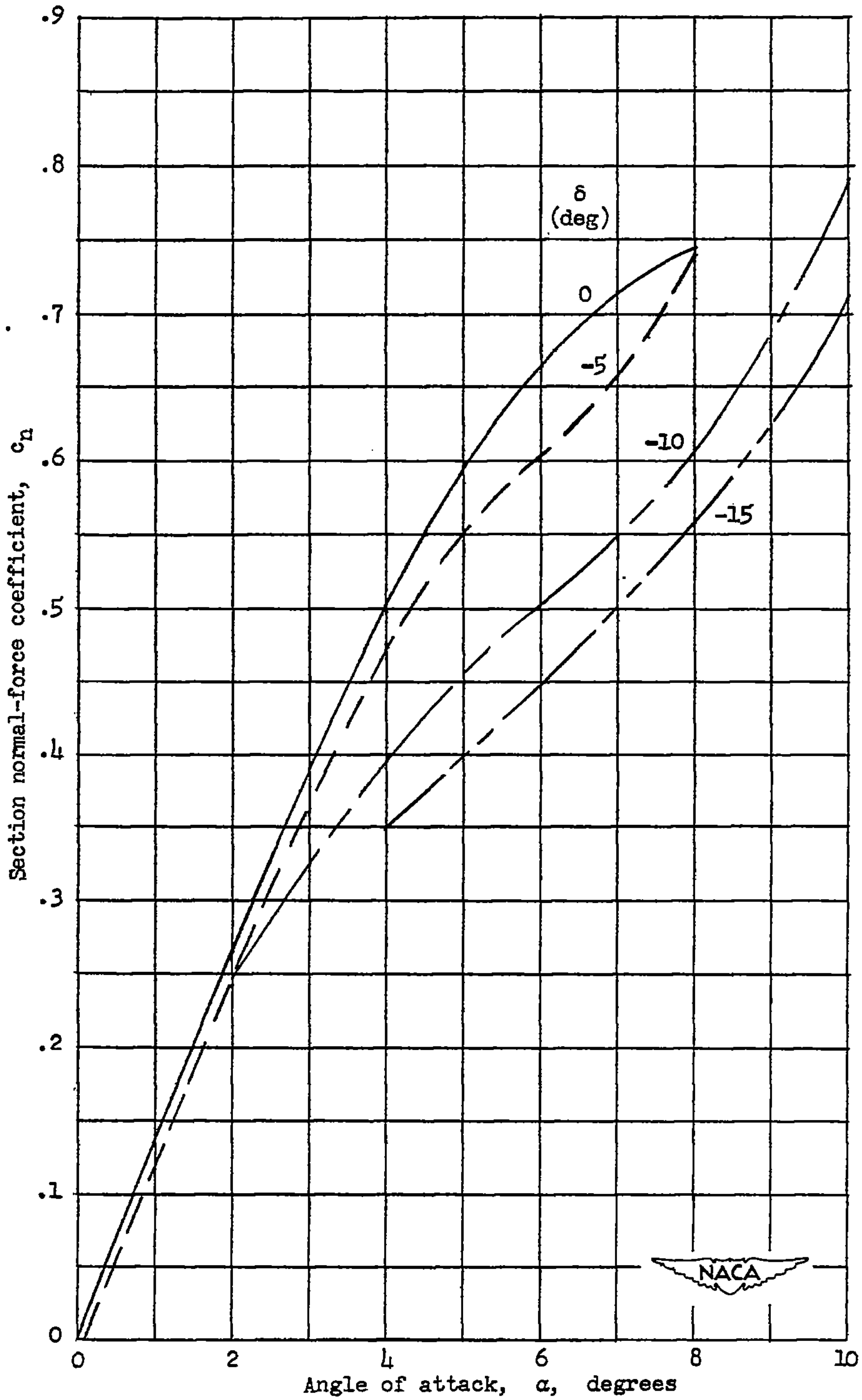

(f) M = 0.9.

Figure 7.- Continued.

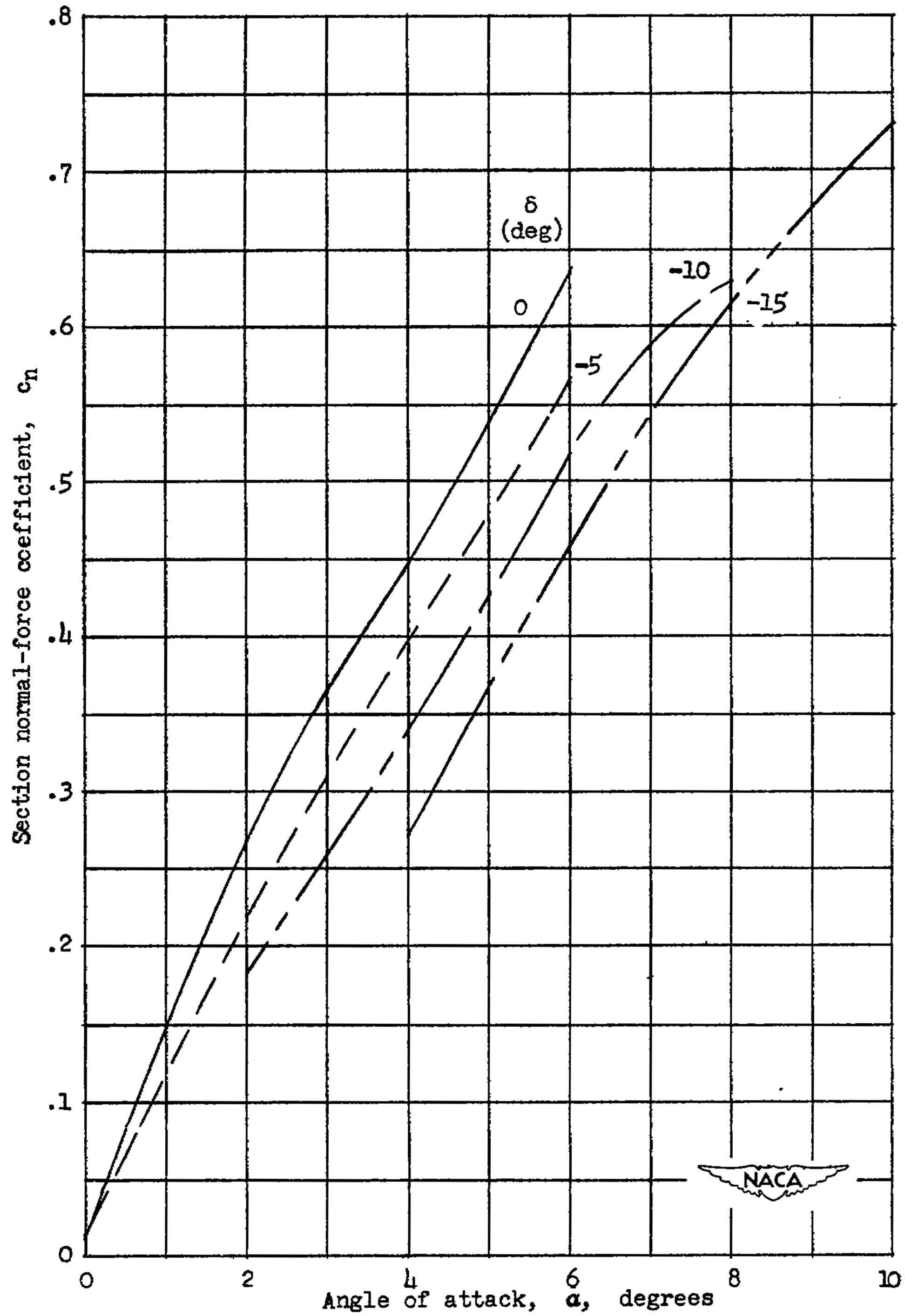

(g) $M = 0.95$.

Figure 7.- Continued.

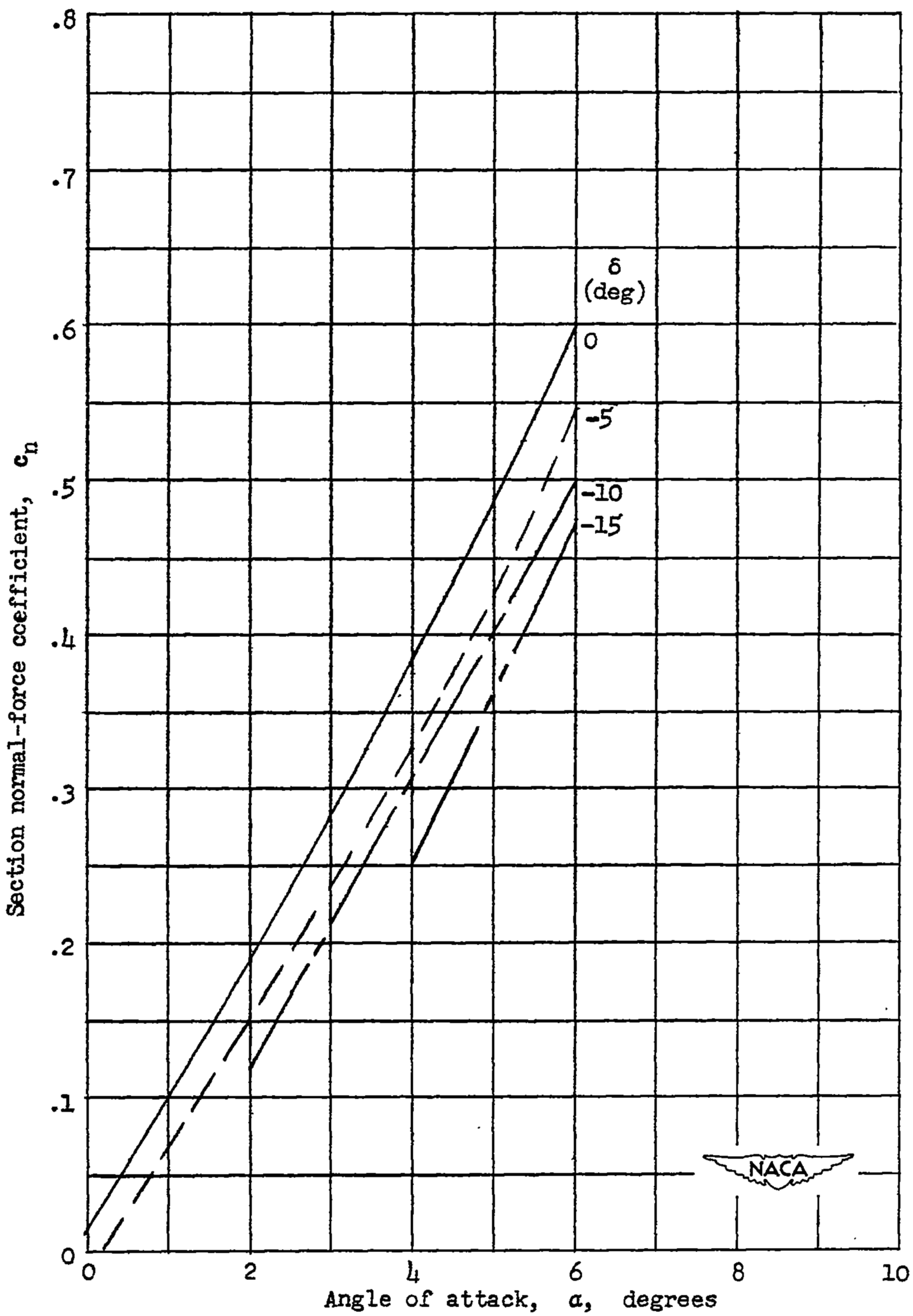

(h) M = 1.0.

Figure 7.- Concluded.

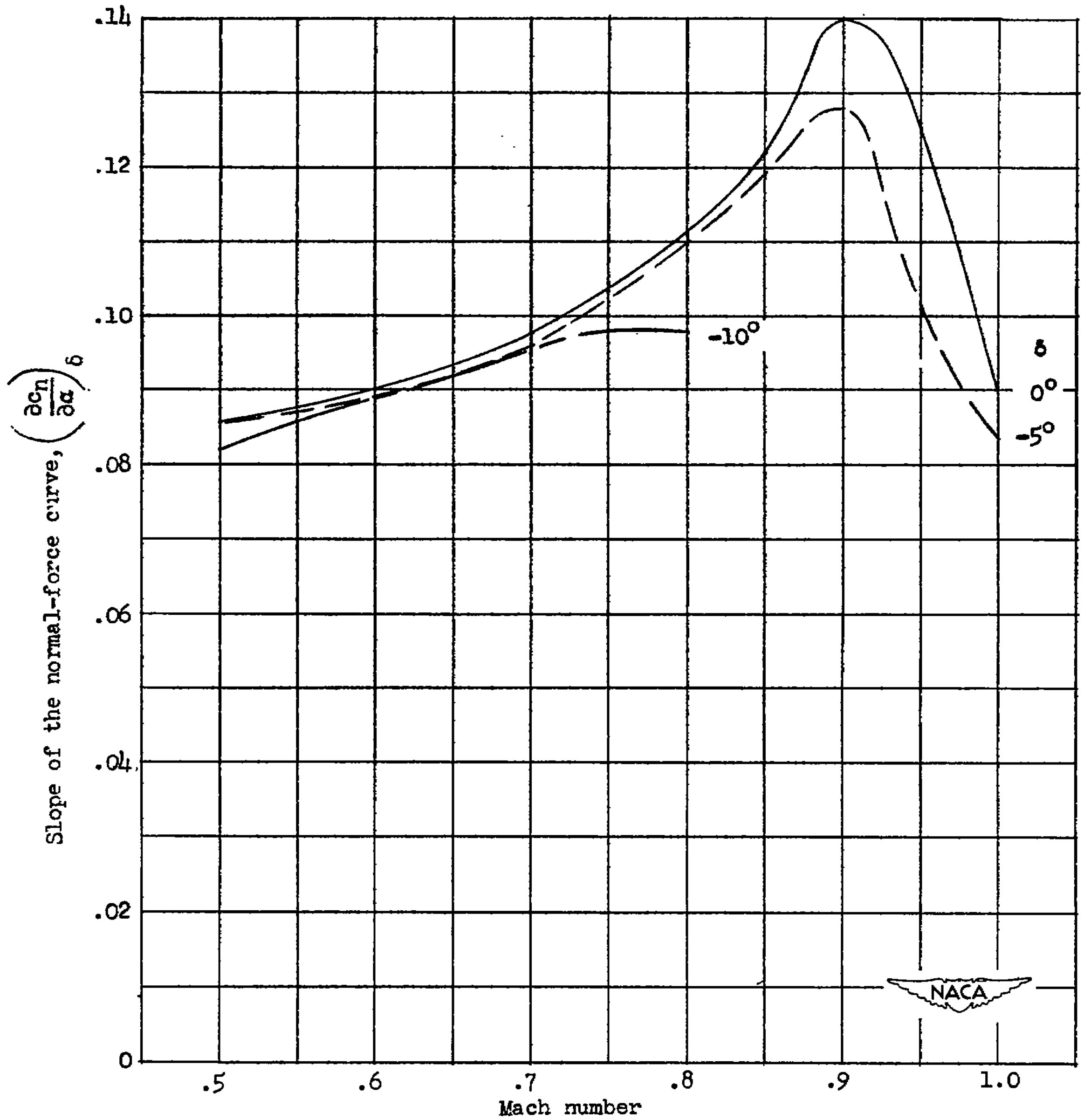

Figure 8.- The effect of leading-edge-flap deflection and Mach number on the slope of the normal-force curve. $\alpha = 0^\circ$ to 5°.

[redacted]

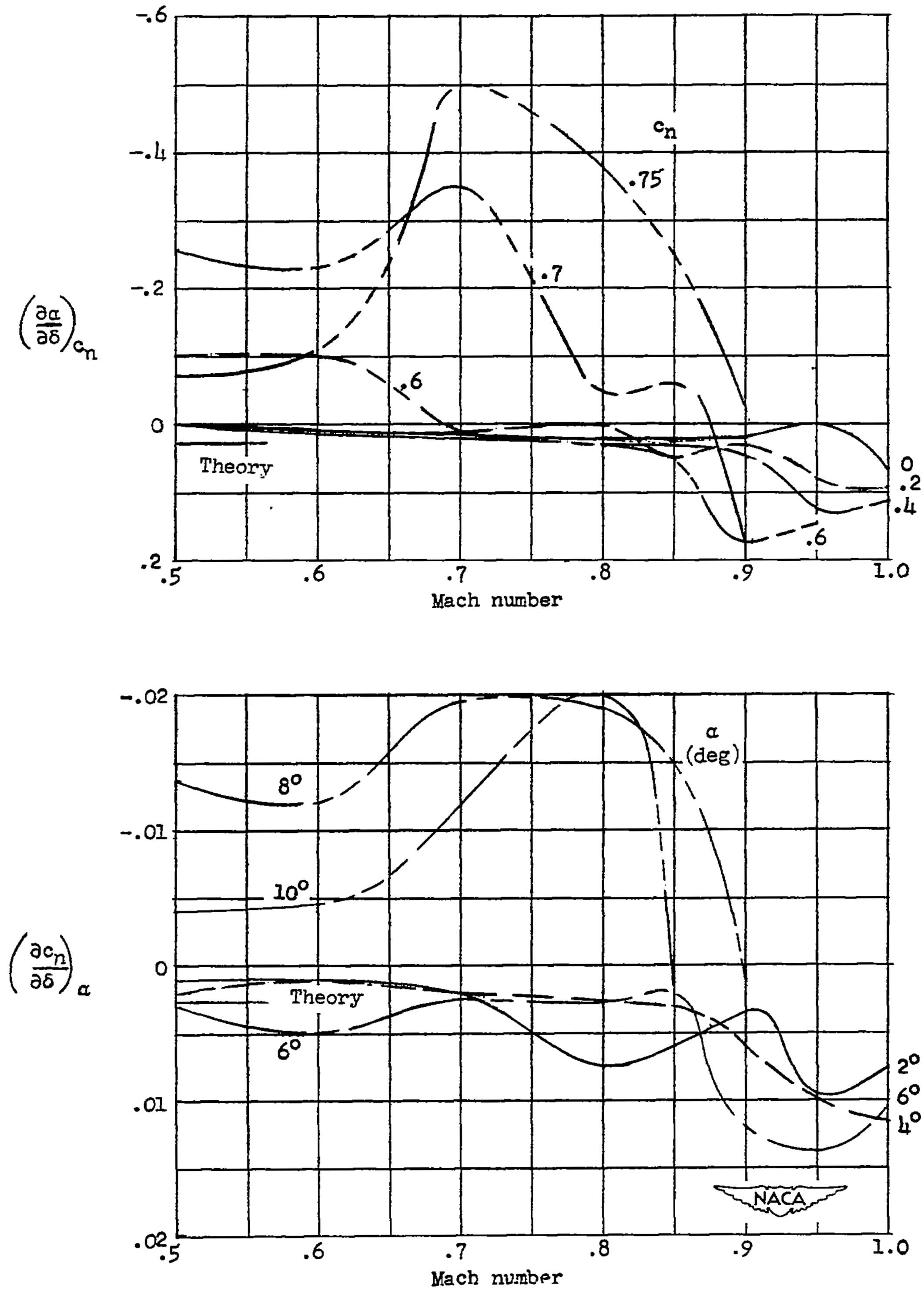

Figure 9.- Flap-effectiveness parameters shown as functions of Mach number. $\delta = 0^\circ$ to -5°.

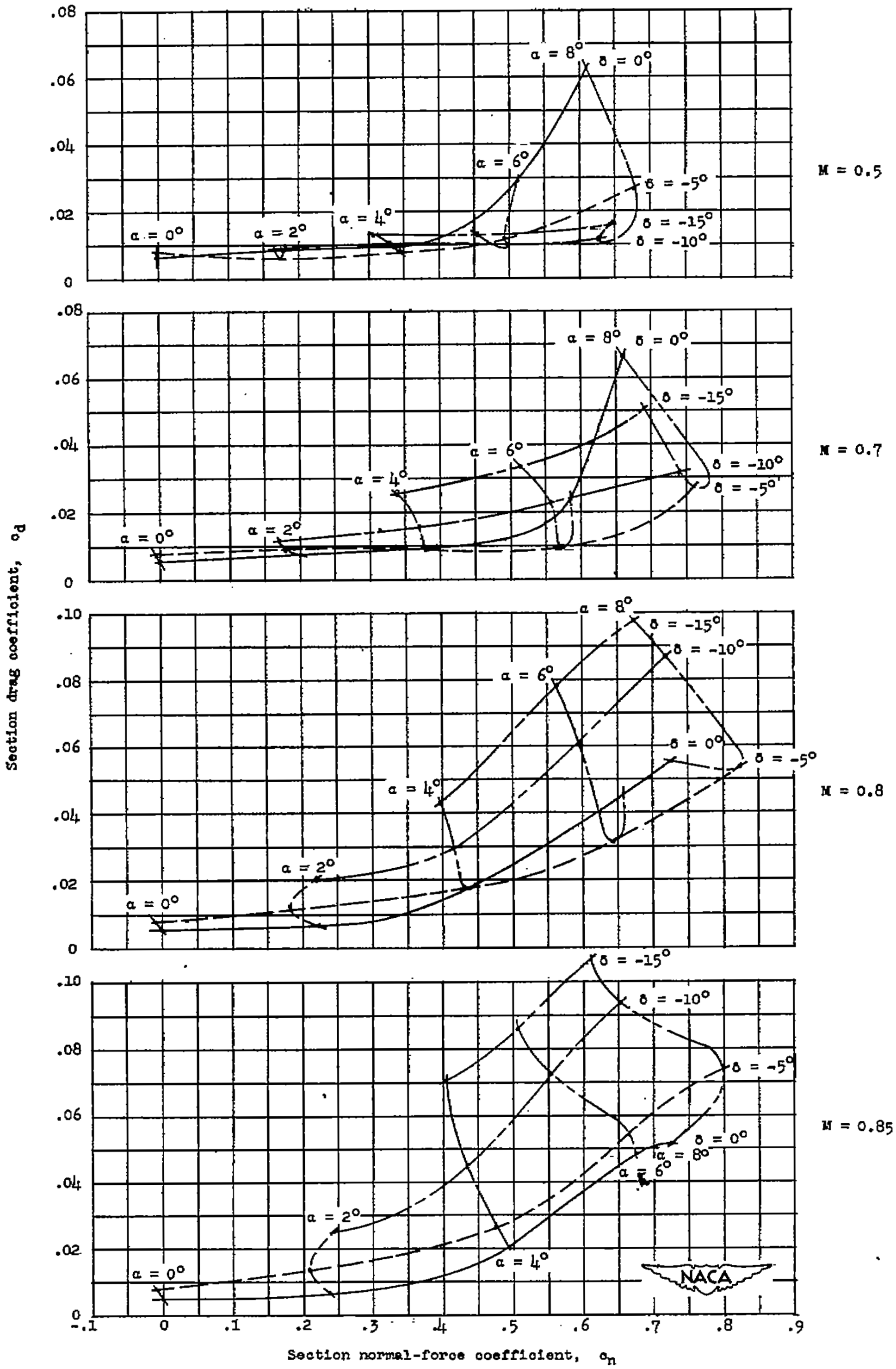

Figure 10.- The effect of leading-edge-flap deflection on the section normal-force and drag coefficients.

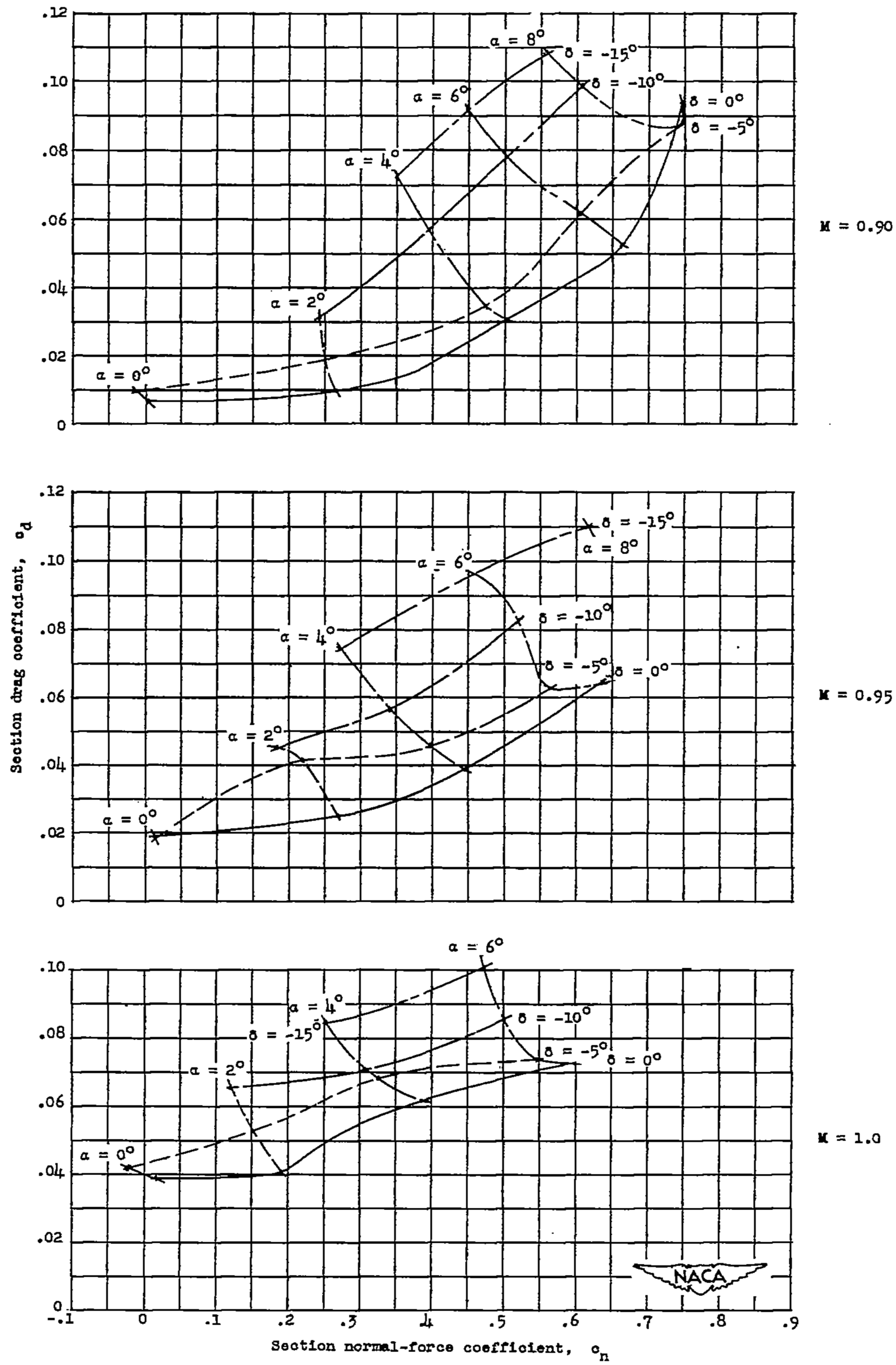

Figure 10.- Concluded.

[redacted]

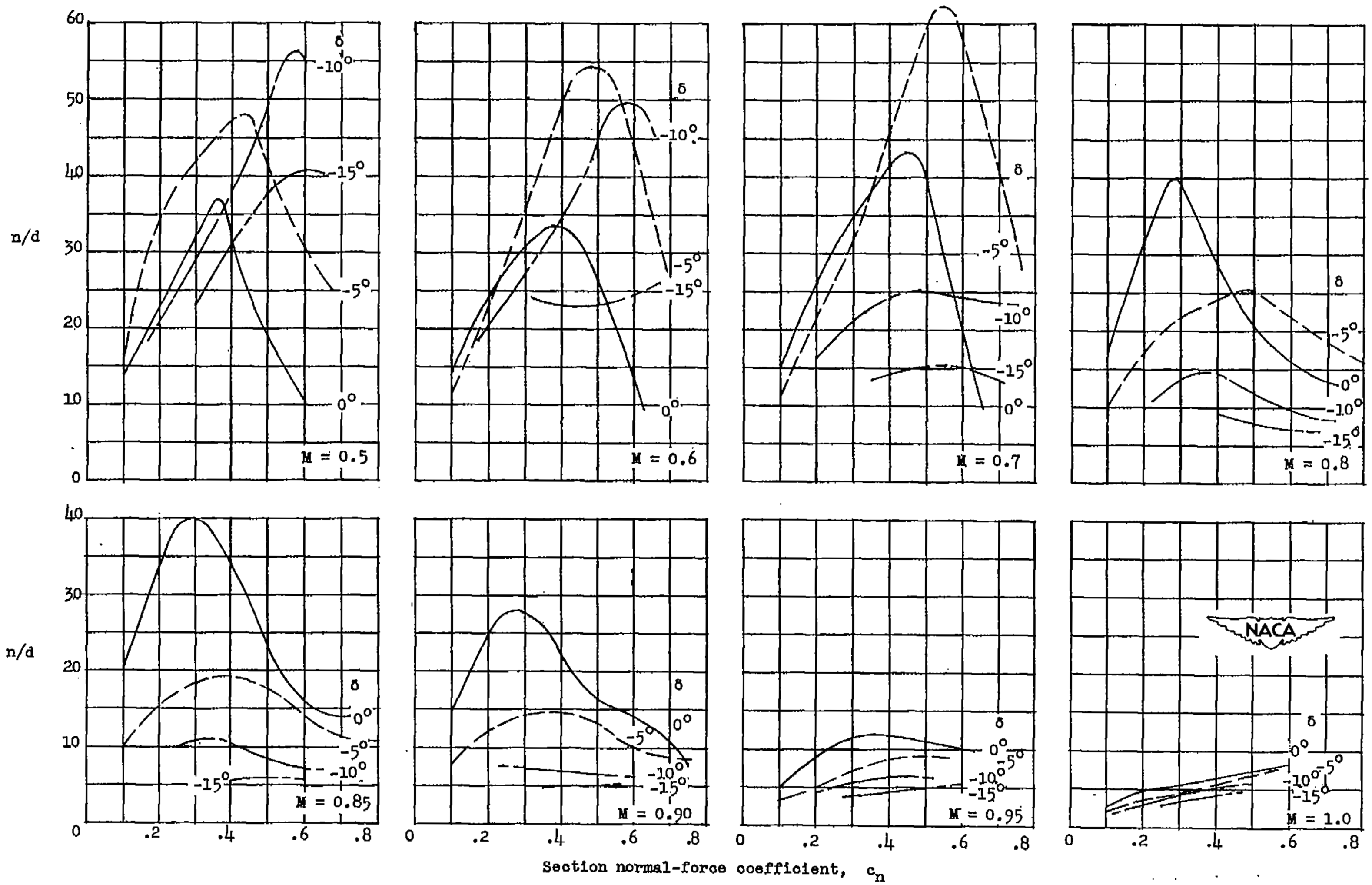

Figure 11.- The effect of leading-edge-flap deflection on the ratio of normal-force to drag at several Mach numbers.

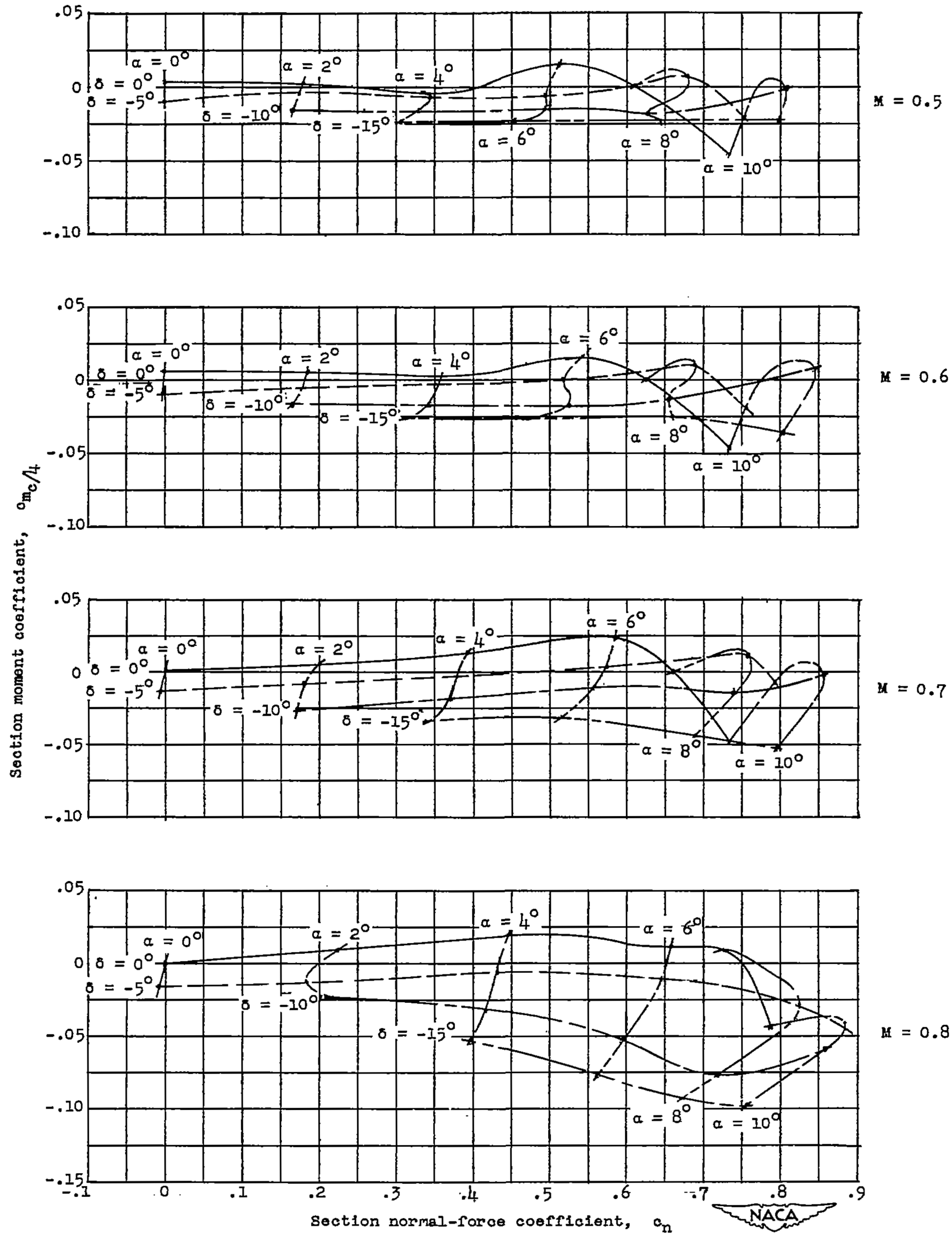

Figure 12.- The effect of leading-edge-flap deflection on the section moment coefficient.

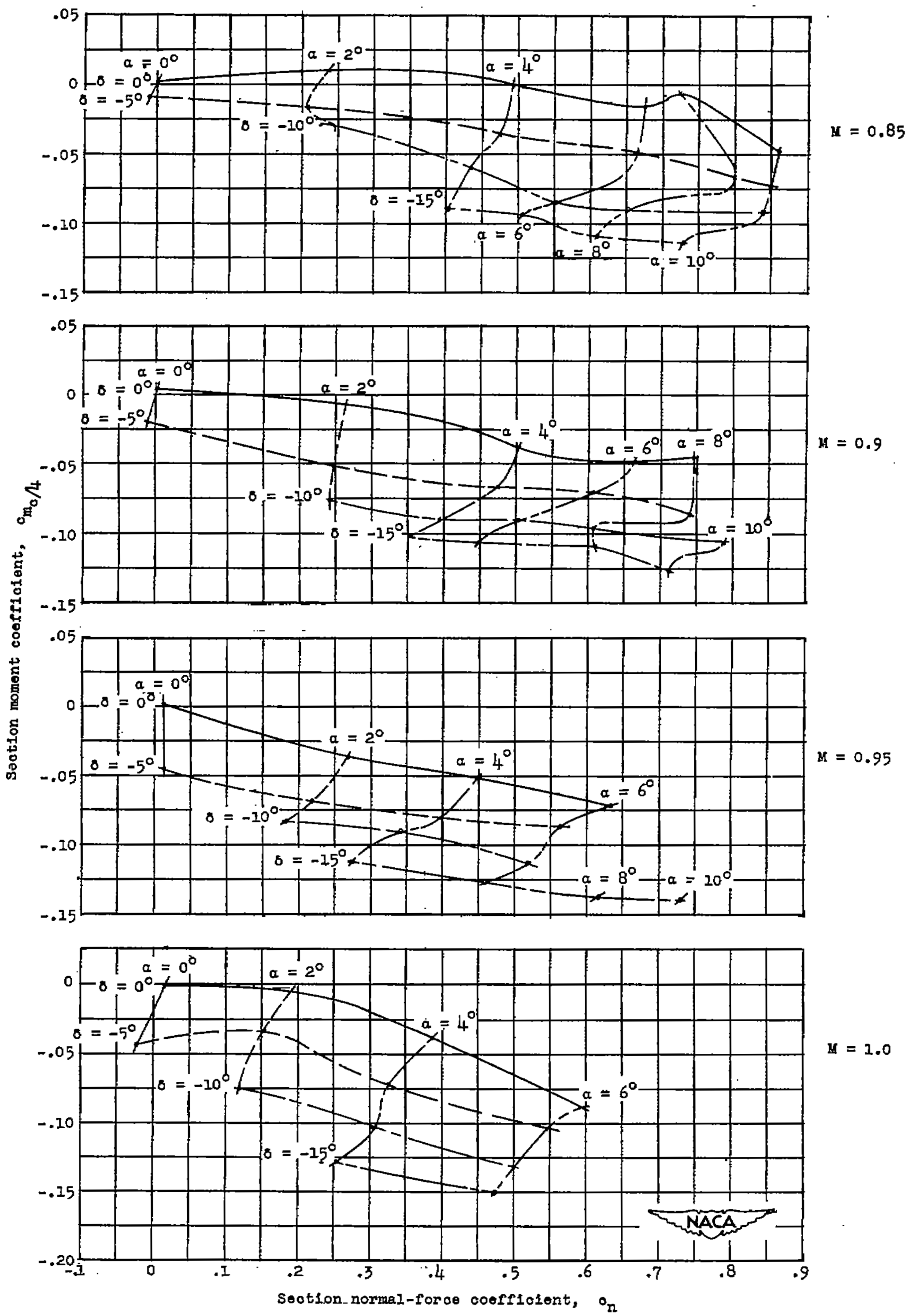

Figure 12.- Concluded.

[redacted]

[redacted]

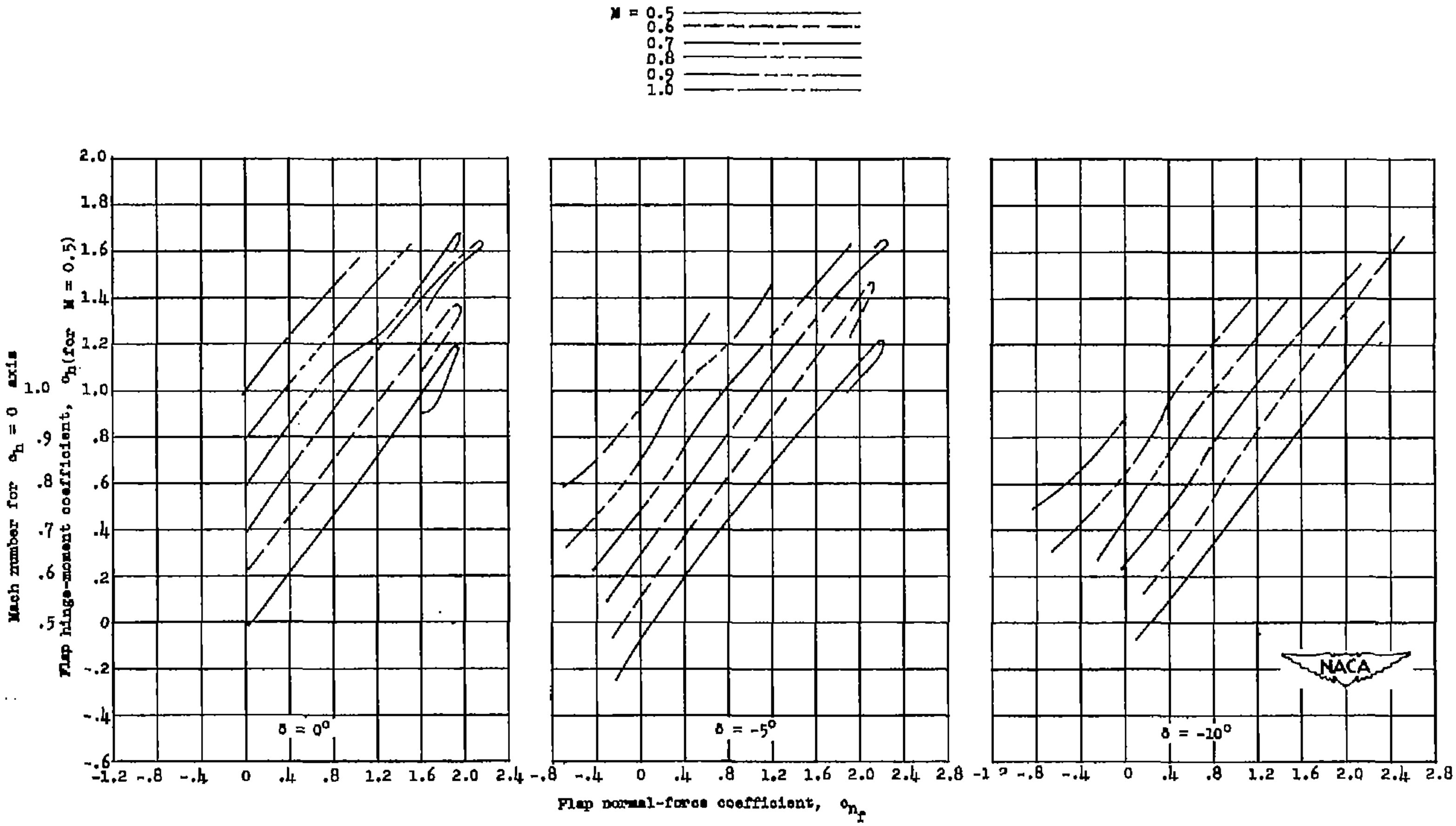

Figure 13.- The variation of flap hinge-moment coefficient with flap normal-force coefficient.

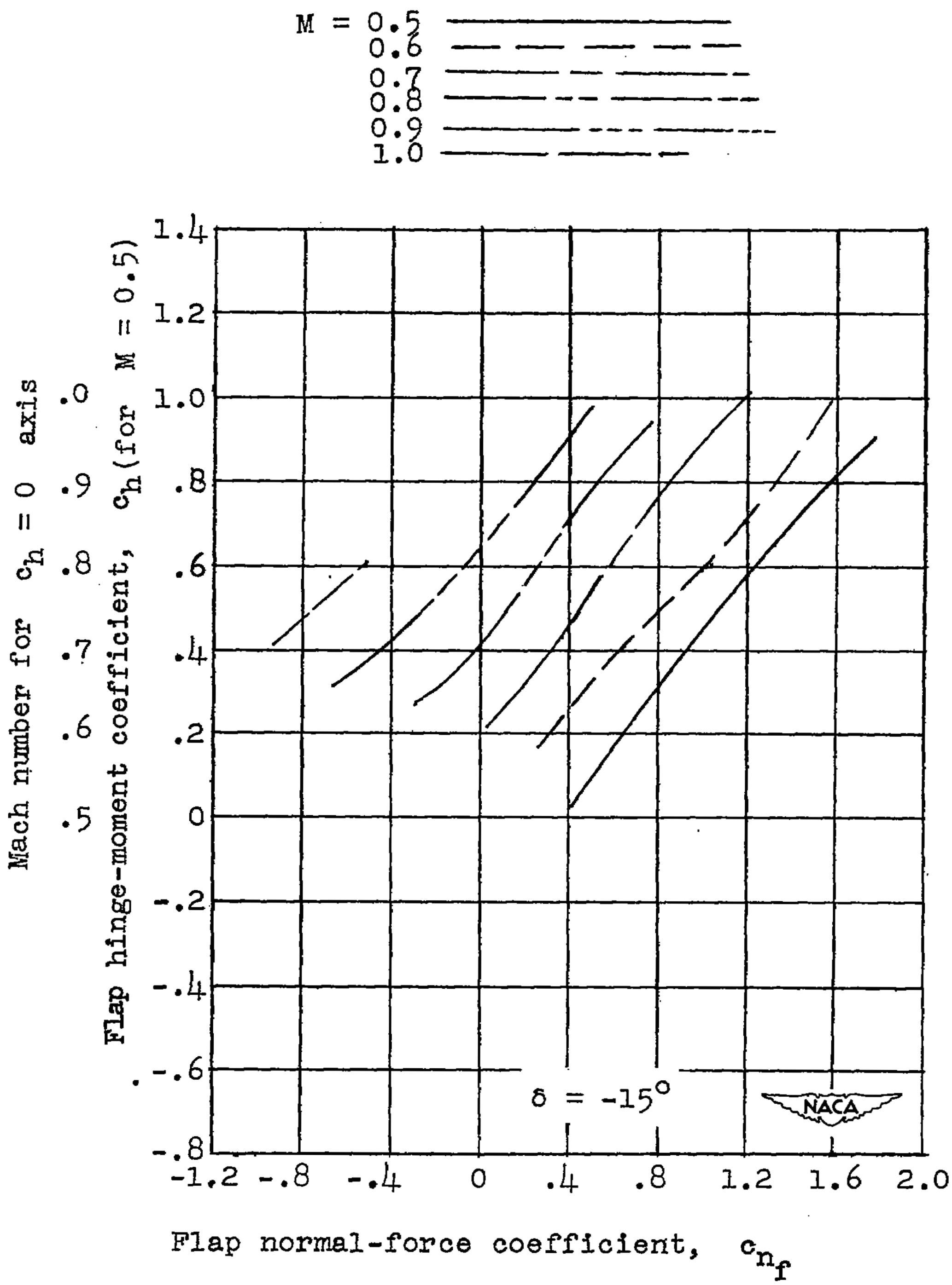

Figure 13.- Concluded.

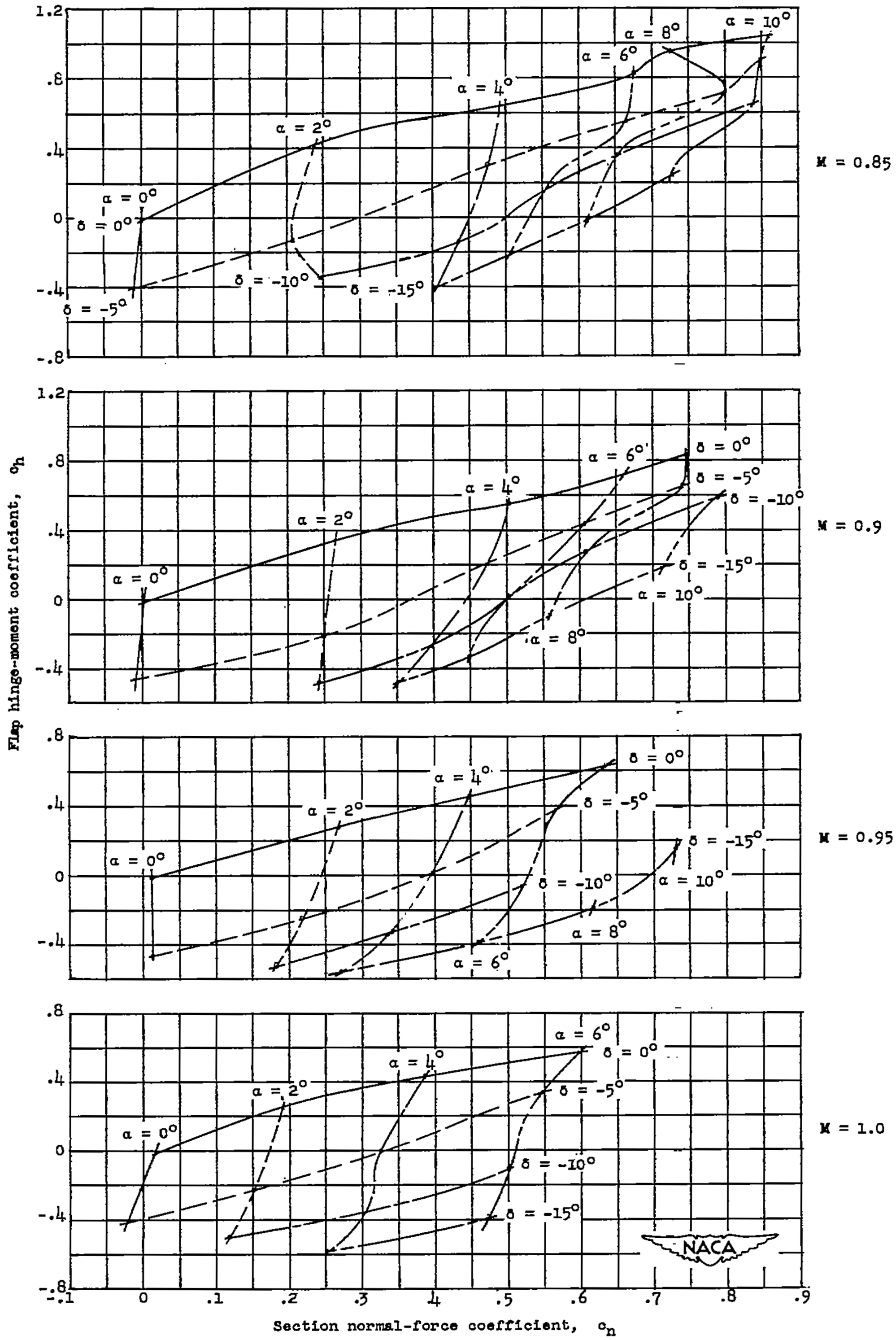

Figure 14.- Concluded.

[redacted]

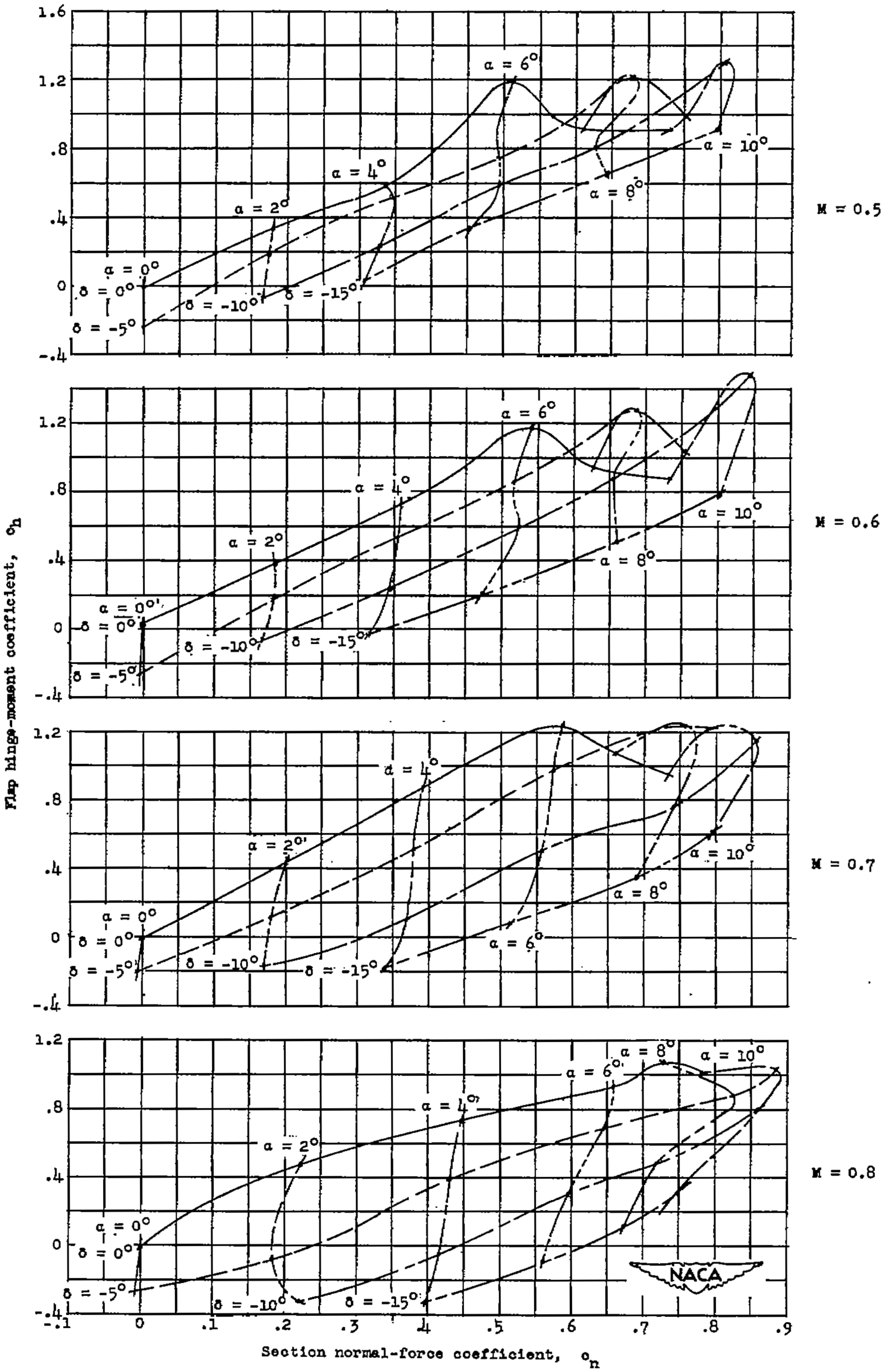

Figure 14.- The effect of leading-edge-flap deflection on flap hinge-moment coefficient.

[redacted]

SECURITY INFORMATION

[redacted]